Canadian Institute of
Guided Ground Transport
Queen's University
at Kingston, Ontario

prepared for
Transportation Development Centre

by
S.T. Lamson
C.A. Dixon

CIGGT Report No. 85-17
Transport Canada Report No. TP-7417E

CA2 ON
UQU 325
85
R17
c.2

86-05774/

CIGGT Project No. PRO-313

CIGGT Report NO. 85-17
Transport Canada Report No. TP-7417E

Library and Information Centre / Centre de documentation (GSLA)
RECEIVED - REÇU LE
JUL 17 1986
Transport Canada / Transports Canada

CIGGT TRACK RESEARCH PROGRAM

Interim Report

November 1984-November 1985

prepared by

S.T. Lamson
C.A. Dixon

for

Transportation Development Centre, Transport Canada

Canadian Institute of Guided Ground Transport
Queen's University, Kingston, Ontario
K7L 3N6

February 1986

Un sommaire en français de ce document est inclus avant la table des matières.

This report resulted from research conducted through the Canadian Institute of Guided Ground Transport. The report represents the views of the authors and does not necessarily have the endorsement of the University or the other participating organizations.

REPORT DOCUMENTATION FORM

1. Transport Canada Report No.	2. TDC Project No	3. Recipient's Catalogue No.
TP-7417E	6059	

4. Title and Subtitle	5. Report Date
CIGGT TRACK RESEARCH PROGRAM Interim Report - November 1984-November 1985	February 1986
	6. Performing Organization Report No. 85-17
7. Author(s) S.T. Lamson and C.A. Dixon	8. Transport Canada File No. D1465-401-2
9. Performing Organization Name and Address Canadian Institute of Guided Ground Transport (CIGGT) Queen's University Kingston, Ontario K7L 3N6	10. DSS File No. 11SD.T8200-3-3524
	11. DSS or Transport Canada Contract No. OSD 83-00120
12. Sponsoring Agency Name and Address Transportation Development Centre (TDC) 200 Dorchester Blvd W., Suite 601, West Tower Montreal, Quebec H2Z 1X4 CN Rail, P.O. Box 8100 Montreal, Quebec H3C 3N4	13. Type of Report and Period Covered Interim - 11/84-11/85
	14. Sponsoring Agency Code TDC 6059
15. Supplementary Notes	16. TDC Project Officer W. Rowan

17. Abstract

The relationship between traffic loading and track response was formulated based on current knowledge of vehicle dynamics and track behaviour. Computer programs thus produced are useful tools for analysis of track maintenance requirements and costs. This report outlines the track system approach to track and component response as a function of traffic loading. The track system computer model is comprised of four modules: vehicle dynamics model, rail life model, tie life model, and surfacing model. Current status of geotextile and subballast design guidelines are also discussed.

18. Key Words	19. Distribution Statement
Track dynamics, Vehicle dynamics, Wheel load, Impact, Equivalent cycle, Track geometry, Settlement, Rail, Tie, Geotextile, Subballast, Rail profile grinding	Available from CIGGT or TDC

20. Security Classification (of this report)	21. Security Classification (of this page)	22. No. of Pages	23. Price
unclassified	unclassified	12 + append.	

FORMULE DE DOCUMENTATION POUR RAPPORT

1. N° du rapport Transports Canada	2. N° de l'étude — CDT	3 N° de catalogue du destinataire
TP-7417E	6059	

4. Titre et sous-titre	5. Date du rapport
CIGGT TRACK RESEARCH PROGRAM Interim Report - November 1984-November 1985	Fevrier 1986
	6. N° du rapport de l'organisme exécutant 85-17
7. Auteur(s) S.T. Lamson and C.A. Dixon	8. N° de dossier Transports Canada D1465-401-2
9. Nom et adresse de l'organisme exécutant Canadian Institute of Guided Ground Transport (CIGGT) Queen's University Kingston, Ontario K7L 3N6	10. N° de dossier — ASC 11SD.T8200-3-3524
	11. N° de contrat — ASC ou Transports Canada OSD 83-00120
12. Nom et adresse de l'organisme parrain Centre de développement des transports (CDT) 200 o., boul. Dorchester, Suite 601, tour ouest Montreal, Québec H2Z 1X4 CN Rail, C.P. 8100 Montréal, Québec H3C 3N4	13. Genre de rapport et période visée Intérim - 11/84-11/85
	14. Code de l'organisme parrain TDC 6059
15. Remarques additionnelles	16. Agent de projet — CDT W. Rowan

17. Résumé

Ce rapport montre le lien entre les charges imposées aux voies ferrées et les réactions de celles-ci, mettant à profit les connaissances acquises en matière d'interaction roue-rail. Les programmes de calcul informatisés qui ont pu être formulés se sont révélés très utiles pour définir les critères de maintenabilité des voies et pour estimer les coûts. Le rapport explique l'approche suivie pour déterminer les réactions des voies et de ses éléments en fonction des charges imposées. Le modèle informatique élaboré comporte les quatre modules suivants : module de la dynamique des véhicules, module de durée de vie des rails, module de durée de vie des traverses et module sur les défauts de nivellement. Le rapport aborde enfin les lignes directrices concernant la conception des géotextiles et de la couche d'assise.

18. Mots-clés	19. Diffusion
Dynamique des voies, dynamique des véhicules, charge de roue, impact, cycle équivalent, géométrie, tassement, traverse, rail, géotextile, couche d'assise, meulage, reprofilage des rails	S'adresser au Centre de développement des transports ou au Canadian Institute of Guided Ground Transport

20. Classification de sécurité (de ce rapport)	21. Classification de sécurité (de cette page)	22. Nombre de pages	23. Prix
non classifié	non classifiée	12 + append.	

TDC 79-005

SUMMARY

The Track Research Program at CIGGT has aimed at developing: (a) practical and cost-effective techniques to reduce track geometry and component deterioration, and (b) a systematic approach to track maintenance planning to improve cost and time efficiency. At the same time, the program also aims to foster basic track support and structure research to ensure the researcher's long-term ability to support track maintenance innovations.

The Track Research Program centres on i) component improvement and ii) track system modelling. The focus of component improvement has been geotextiles, subballast and tie/fastener systems. Geotextiles and subballast research has contributed to improved track design and construction. Tie/fastener system research centred on the degradation of wood ties and the merits of changing to concrete or steel ties.

The track system model links vehicle dynamic force inputs (from mixed traffic) experienced by the track to the deterioration of track components and geometry. A vehicle of a given design, running over a track section of a given standard, at a given speed, will create a spectrum of track forces.

These forces are transmitted into the track, causing wear and fatigue to track components and deterioration of track geometry. The distribution of these forces depends on track design and the condition of the track components. Repair and replacement costs are incurred due to component wear and fatigue. Deterioration of track geometry increases track errors and leads to larger dynamic wheel loads as subsequent trains pass. This cycle continues until track components and geometry are reconditioned, and the track deterioration process is generally self-accelerating.

A track system model consisting of four modules has been developed. The modules are:

- Vehicle Dynamics Model
- Rail Life Model
- Tie Life Model
- Surfacing Model

The Vehicle Dynamics Module produces key components of the dynamic load for each set of traffic/track conditions in a mixed traffic operation. Outputs from this module are fed to the Rail, Tie and Surfacing Modules to calculate track component and geometry degradation and maintenance costs.

SOMMAIRE

Le programme de recherche du CIGGT sur la tenue des voies ferrées vise le double but suivant : a) étudier des techniques fiables et économiques en vue d'atténuer la dégradation de la géométrie des voies ferrées et de ses éléments, et b) dégager une méthode de planification systématique de la maintenance débouchant sur un accroissement de l'efficacité des interventions et une diminution des coûts correspondants. En outre, ce programme vise à encourager la recherche de base pour déboucher à long terme sur des techniques novatrices susceptibles d'améliorer la maintenabilité des infrastructures.

Pour réaliser son programme, le CIGGT s'est concentré sur : i) l'amélioration des éléments de la voie et ii) la modélisation des facteurs en jeu. En ce qui concerne les voies, le CIGGT a pris en compte les géotextiles, la granulométrie de la couche d'assise et les systèmes traverses-fixations. La recherche sur les géotextiles et la granulométrie a débouché sur la réalisation de voies mieux conçues et mieux construites. Côté systèmes de fixation, la recherche a été axée sur les conditions de dégradation des traverses en bois et sur les avantages des traverses en béton et en acier.

Par l'autre approche, celle de la modélisation, la recherche vise à établir la corrélation entre les charges imposées aux voies par des matériels de catégories différentes et les avaries qui en découlent, tant pour les éléments de la voie que pour la voie entière elle-même. On sait qu'un matériel d'un certain modèle, circulant à une vitesse donnée sur un tronçon ayant des caractéristiques connues suscite des efforts dont le spectre est comparable à nul autre.

Ces efforts ont pour effet de détériorer la voie par usure et fatigue des éléments et de provoquer des déformations géométriques. Quant à la distribution de ces efforts, elle dépend de la construction de la voie et de l'état de ses éléments. L'effet de l'usure et de la fatigue est de nature financière : coûts de réparation et de remplacement. L'effet des déformations est double : aggravation des défauts existants et accroissement des charges dynamiques exercées par les roues à chaque passage de train. On reconnaît là un cercle vicieux qui ne s'interrompt qu'avec la réflection des voies.

Pour mettre en rapport tous les facteurs en jeu, un modèle mathématique a été élaboré, comportant les quatre modules suivants :

- dynamique des véhicules
- durée de vie des rails
- durée de vie des traverses
- défauts de nivellement.

Le premier module calcule les charges engendrées par chaque combinaison de trafic, de voie et de matériel, les données en sortie alimentant ensuite les autres modules qui convertissent à leur tour ces données en avaries correspondantes et en coût de maintenance.

TABLE OF CONTENTS

1. INTRODUCTION 1

2. PROGRESS IN TRACK COMPONENT IMPROVEMENT RESEARCH 3

3. PROGRESS ON TRACK SYSTEM MODEL DEVELOPMENT 5
   - 3.1 Scope of Work 5
   - 3.2 Current Status 11

4. FURTHUR WORK 11
   - 4.1 Vehicle Dynamic Model 11
   - 4.2 Rail Life Model 11
   - 4.3 Tie Life Model 11
   - 4.4 Surfacing Model 12
   - 4.5 Track System Model 12

Appendix A: DEVELOPMENT OF AN EMPIRICAL RELATIONSHIP FOR VERTICAL DYNAMIC WHEEL FORCE VARIATION OF A 100-TON CAR AS A FUNCTION OF TRACK ROUGHNESS AND VEHICLE SPEED

Appendix B: RAIL LIFE MODEL

Appendix C: SURFACING MAINTENANCE COST MODEL

Appendix D: SAMPLE LOTUS 1-2-3 WORK SHEET

LIST OF FIGURES

1. Track system 5

2. Track System Maintenance Cost Model 8

1. INTRODUCTION

Canadian railways have experienced a rapid increase in traffic growth during the last two decades. This increase has been accommodated by a large increase in axle loads, train speeds and train lengths, as well as some modest track capacity expansionary construction. On some of the most heavily loaded lines, the railways have made significant investments in track upgrading to offset accelerated wear rates.

It is expected that traffic growth will continue. This creates demand for further increases in axle loads, train lengths and traffic density, since track capacity expansionary construction is very costly. The Australian iron ore railways recently experimented with a train length of 230 cars, an axle load of 35 tonnes and a speed of 85 km/h. In North America there has been a great deal of contemplation about using 125-ton cars (approximately 35 tonnes axle load) for freight traffic and a speed of 200 km/h (125 mph) for passenger traffic. Rail, tie wear and track geometry deterioration are likely to increase, creating a greater requirement for track maintenance, precisely when less track occupancy time for maintenance can be made available.

Tighter operating conditions and increasing competitiveness among North American railroads has led to the need for more effective management tools to aid in the decision-making process. For a long time railroads have used computer technology to develop extensive data bases on track performance. Information is now available on the degradation history and current status of track components and geometry. Information is also available on the related traffic characteristics. A computer program which links traffic to track degradation would be very helpful in assisting the railroads to make better use of available information. With the recent development of microcomputers, such tools can now be used not only by head office management but also by local track maintenance managers to improve the overall productivity.

The Transportation Development Centre of Transport Canada has sponsored a three-year government/industry cooperative track system research program aimed at developing (a) practical and cost-effective techniques to reduce track geometry and component deterioration, and (b) a systematic approach to track maintenance planning to improve cost and time efficiency. At the same time, the program also aims to foster

basic track support and structure research to ensure the researcher's long-term ability to support track maintenance innovations.

Railway industry support was provided by CN Rail, CP Rail, and the Association of American Railroads, either as direct or parallel project support.

This report describes the achievements of the program at the end of the second year and outlines the work plan for the final year.

2. PROGRESS IN TRACK COMPONENT IMPROVEMENT RESEARCH

The principal achievements of the track component research program to date are specifications and design guidelines for effective application of geotextiles and subballast in track structure construction and rehabilitation.

The geotextile specifications cover not only the desirable material properties but also the procedure and apparatus used in qualification testing and the manufacturing process which can yield the basic required properties. The design guidelines for geotextiles cover installation procedures and track locations where geotextiles will offer the greatest improvement potential.

The specification on subballast covers track design options with and without geotextiles. Together with earlier comprehensive research on ballast which led to the development of modern ballast specifications at CN and CP, recent work provides the basis for significant improvement in the design and construction of the track support structure. A comprehensive report on the subject has been produced by the principal researcher, Dr. G.P. Raymond of Queen's University in Kingston.[1]

In addition to research on track support, two other parallel research programs at CIGGT deserve mention. One concerns rail profile grinding, the other tie/fastener systems.

The rail profile grinding research program,[2] under way since 1981, has resulted in new ground rail profile specifications which, as indicated by field trial data, could save significant rail costs. This program is now moving into the third phase which concentrates on practical procedures to extract the most benefit from the new grinding technique.

---

1 "Subballast and Geotextiles for Track Support Separation Applications," G.P. Raymond, CIGGT Report No. 85-12, December 1985.

2 "Rail Profile Grinding," S.T. Lamson, CIGGT Report 82-7, November 1982; "Rail Profile Grinding -- Phase II," S.T. Lamson, CIGGT Report No. 84-14, February 1985.

The tie/fastener system program,[3] in progress since 1985, examines the degradation process of wood ties and the merits of changing to concrete or steel ties. Results of work to date have identified a number of improvements which could significantly extend the life and performance quality of wood ties. The cost/performance trade-offs of steel and concrete ties were analyzed. This program is now moving into the second phase which concentrates on the influence of fastening system elasticity on track performance. The initial work will examine the steel tie.

---

3 "Assessment of Steel Railway Ties," M.L. Driscoll, S.T. Lamson, CIGGT Report No. 85-8, October 1985.

3. PROGRESS IN TRACK SYSTEM MODEL DEVELOPMENT

3.1 Scope of Work

Figure 1 is a schematic diagram of the track system. It describes the main interactive processes which link the vehicle dynamic force inputs experienced by the track to the deterioration of track components and geometry. As shown, a vehicle of a given design, running over a track section of a given standard, at a given speed, will create a spectrum of track forces.

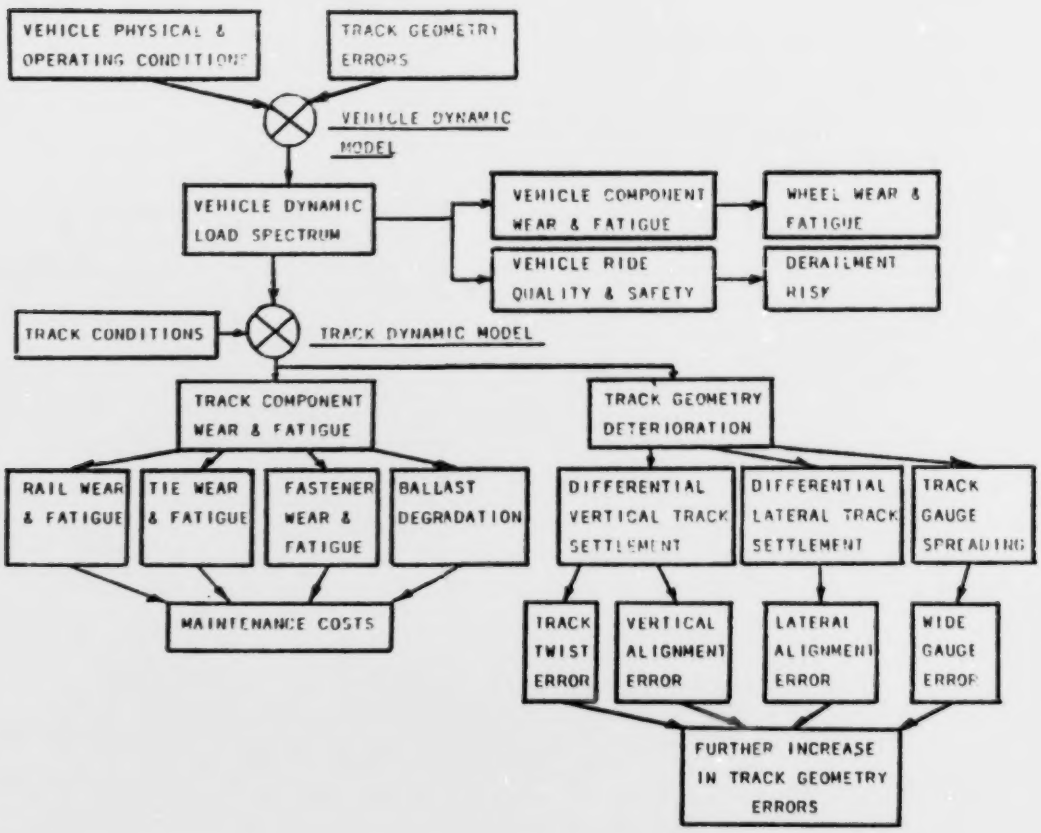

Figure 1 Track system

These forces are transmitted into the track, causing wear and fatigue of track components and deterioration of track geometry. The distribution of these forces depends on track design and the condition of the track components. Repair and replacement costs are incurred due to component wear and fatigue. Deterioration of track geometry increases track errors and leads to larger dynamic wheel loads as subsequent trains pass. This cycle continues until track components and geometry are reconditioned. Thus, vehicle performance and track response are inter-related, and the track deterioration process is generally self-accelerating.

To understand and quantify the behaviour and interaction of such systems, the following work must be carried out:

(a) **Determination of track loading.** Each type of vehicle in a traffic mix, operating at a given speed, generates a unique dynamic wheel load spectrum. The variation of load within a spectrum is due to the random variation of physical properties within a vehicle type (e.g. wheel geometry defects) and the random variation of track geometry within a track section (e.g. surface roughness). Therefore, representing each type of vehicle by its static axle load or static axle load modified by an impact factor based on speed and wheel diameter as conventionally done in North America is very inadequate. For each vehicle type in a traffic mix, the necessary track loading information is its dynamic wheel load spectrum. Of this, the minimum information is the steady-state level and dynamic variation of the wheel force in the vertical and lateral direction.

(b) **Determination of track response.** For any given set of dynamic wheel forces from given traffic, there is a corresponding set of forces on ties and ballast. This load distribution varies with track configuration and track component conditions. One common technique for estimating load distribution is based on the theory of beam (rail) on elastic foundation (ties and ballast). Once the load distribution is known, the deflections and stresses in ballast, sub-ballast and subgrade can be estimated.

(c) **Estimation of track component deterioration rate.** Steps (a) and (b) produce data describing the loading (i.e. forces/stresses) on each track

component. Based on this data, estimates of wear and fatigue rates of track components such as rails and ties can be made. These will indicate the level of track maintenance effort which a given track design would require in the long term under a specified traffic level.

(d) **Estimation of track geometry deterioration rate.** Since conventional track design is not rigid, the continued application of wheel loads leads to track settlement. Further, because wheel forces generally vary along the track, the settlement is not uniform. This leads to further increases in track geometry errors and, in turn, to further increases in wheel forces. Research work in the area of track settlement has resulted in some understanding of track settlement behaviour. This can be used to construct a preliminary model of track differential settlement for use in analyzing track geometry deterioration problems.

3.2 Current Status

A track system model consisting of four modules has been developed. The modules are:

- the Vehicle Dynamic Model
- the Rail Life Model
- the Tie Life Model
- the Surfacing Model.

Figure 2 describes the structure of the model. The Vehicle Dynamic module produces the key components of the dynamic wheel load for each set of traffic/track conditions.

Outputs from this module are fed to the Rail, Tie and Surface modules to calculate track component and geometry degradation and maintenance cost.

A key feature of the model structure is the normalization of the wheel loading cycle. This involves converting the actual number of wheel loading cycles of a given traffic category in a traffic mix into the equivalent number of wheel loading cycles of a reference traffic category.

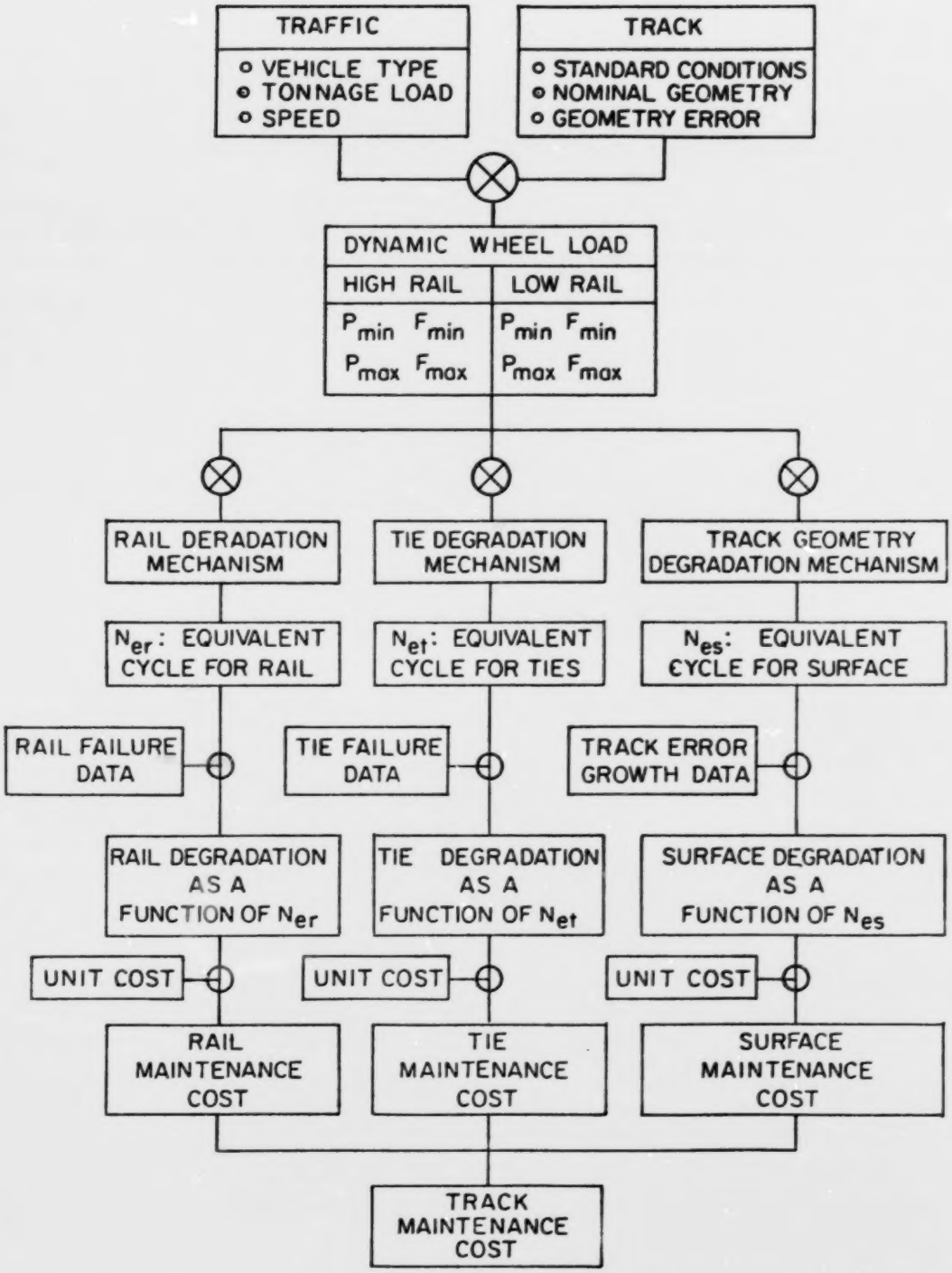

Figure 2 Track System Maintenance Cost Model

The reference traffic category is normally selected to represent the traffic category which contributes the most to the overall track maintenance cost and whose characteristics are most understood. For North American main lines, this is generally the 100-ton car.

The normalization is based on the relative contribution to track degradation by a given traffic category compared to that by the reference traffic. For example, if the wheel loading cycle of a six-axle locomotive causes twice as much differential track settlement as that of a 100-ton car (reference traffic), it is equivalent to two cycles.

This normalization process converts a mixed traffic situation into an equivalent uniform traffic situation. The total equivalent cycles are then compared against the actual failure data to establish an empirical relationship between traffic and track degradation. This empirical relationship can later be applied to future track and/or traffic conditions to predict the future rate of track degradation and maintenance cost. Note that as rail, tie and surface degradation mechanisms are different, the total equivalent cycles for rail, tie and surface will be different, even though the total actual cycle is the same.

This model structure is very flexible. It is designed to make the best use of the existing incomplete understanding of track system performance and degradation processes, as well as the incomplete details of track and traffic data. Essentially, the model will give the best possible answer for a given level of knowledge and information. More knowledge and/or more information can be readily incorporated to give better results. Considering that complete understanding of track behaviour and complete availability of traffic and track data will never be achieved in absolute terms, this is in fact a reasonable strategy.

For ease of trial application, the first version is set up in a Lotus 1-2-3 work sheet format. Appendix D shows a sample work sheet of the program, describing the complete model except for the macro, which performs behind-the-scenes iterations. The constraints of a work sheet format necessitate some simplifications, and hence reduced accuracy. However, in this format the model can be run on a microcomputer by an operator with no programming background.

Arrangements have been made to test this model against a real track maintenance environment at the subdivision level in the near future.

It should be noted that the individual modules of the model have been applied to analysis of some aspects of track maintenance on a number of operating railroads. These will continue to be upgraded as further research findings become available. Details are given in the following section.

4. FURTHER WORK

4.1 Vehicle Dynamic Model

Appendix A describes the current level of development in estimating dynamic wheel load. The progress made since the last interim report (November 1983-November 1984) includes:

- more simulation runs
- validation of a velocity term using actual Canadian railway wheel impact data.

Arrangements have been made with the AAR to obtain data on dynamic wheel loads from FAST for further validation.

4.2 Rail Life Model

Appendix B describes a new concept of rail life and cost estimation. Various rail degradation mechanisms (e.g. wear, fatigue) from the Rail Wear Cost Model[4] can be extracted and applied to this report. This, however, is not yet fully realized since the Rail Wear Cost Model itself is being completely reviewed and updated by MIT as part of a current MIT/AAR/CIGGT joint research program.

4.3 Tie Life Model

A description of the Tie Life Model was given in the last interim report. Full details are given in the CIGGT report entitled "Tie Life Model."[5] The AAR is currently conducting laboratory loading tests on wood ties and laboratory-induced aging of wood ties. The results of this research, when available, will be used to upgrade the tie degradation mechanism currently employed in the model. Arrangements have been made to extend the calibration of the model with CP data, and to carry out trial applications to assess its usefulness.

---

4 "CIGGT Rail Wear Cost Model: User's Manual," E.R. McIlveen, A.M. Birk, J.D. Young, R. Glaser, CIGGT Report No. 81-19, April 1982.

5 "Tie Life Model," S.T. Lamson, B. Dowdall, CIGGT Report No. 84-12, January 1985.

4.4 Surfacing Model

Appendix C provides a full description of the Surfacing Model.

This model has been calibrated to actual Canadian railway track geometry error data for analysis of track maintenance conditions. Arrangements have been made to carry out a calibration using additional data in the near future.

Arrangements have also been made to obtain track settlement data to further validate the model.

4.5 Track System Model

Concurrent to the upgrading of individual modules, preparatory work is currently being undertaken to set up a more comprehensive system model version on FORTRAN. This version will be more accurate and capable of handling larger calculations.

APPENDIX A

DEVELOPMENT OF AN EMPIRICAL RELATIONSHIP FOR VERTICAL DYNAMIC WHEEL FORCE VARIATION OF A 100-TON CAR AS A FUNCTION OF TRACK ROUGHNESS AND VEHICLE SPEED

A.1 OBJECTIVE

To derive an equation for the dynamic force variation of a 100-ton car as a function of track roughness and vehicle speed.

$$\Delta Pd = f \text{ (track roughness, vehicle speed)}$$

where ΔPd expresses one standard deviation of the dynamic force.

A.2 CONSTRAINTS

Track roughness is expressed as surface index (SI) and cross-level index (CI) since these are currently available.

A.3 METHOD

At present the most reliable method of estimating the dynamic wheel forces as a vehicle responds to track roughness is by computer simulation. Using a full-body vertical dynamic model, the response of a 100-ton car can be simulated for any track location under a range of vehicle speeds. This procedure is shown in Figure A.1(a).

Computer simulation is, however, very time-consuming, and hence not practical for an economic analysis which requires an estimate of the vehicle dynamic wheel forces over long distances of track. To overcome this problem, a quasi-empirical method is used. It involves regression analysis of data generated by computer simulation. The result is a quasi-empirical equation which produces an estimate of the dynamic wheel forces for a given set of track surface and cross-level errors. This procedure is shown in Figure A.1(b).

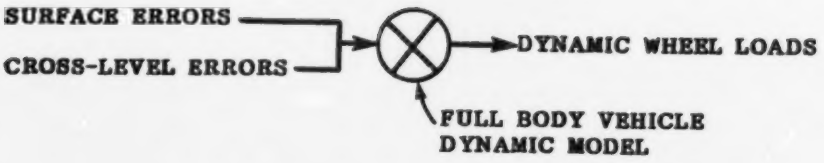

(a) by computer simulation

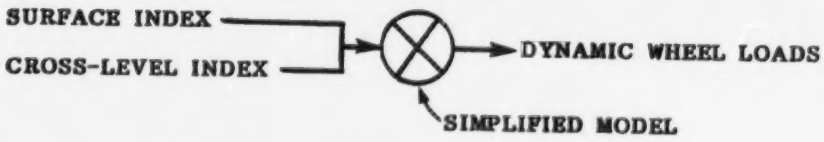

(b) by equation

Figure A.1 Estimation of dynamic wheel loads

The quasi-empirical equation is considered equivalent to the computer simulation for estimating dynamic wheel loads. Note that track roughness input can be represented by track indices. These are readily available for all track; hence the equation is much more versatile than a computer model.

A.4 VEHICLE DYNAMICS COMPUTER MODEL

A.4.1 Description

This model simulates the dynamic response of a four-axle rail vehicle to random surface irregularities as characterized by track coodinates (x,y), rate of change of position (dy/dx), and the second derivative of position (d^2y/dx^2) for both track surface and cross-level conditions. Of prime interest are the dynamic wheel/rail forces. A diagram of the model is shown in Figure A.2.

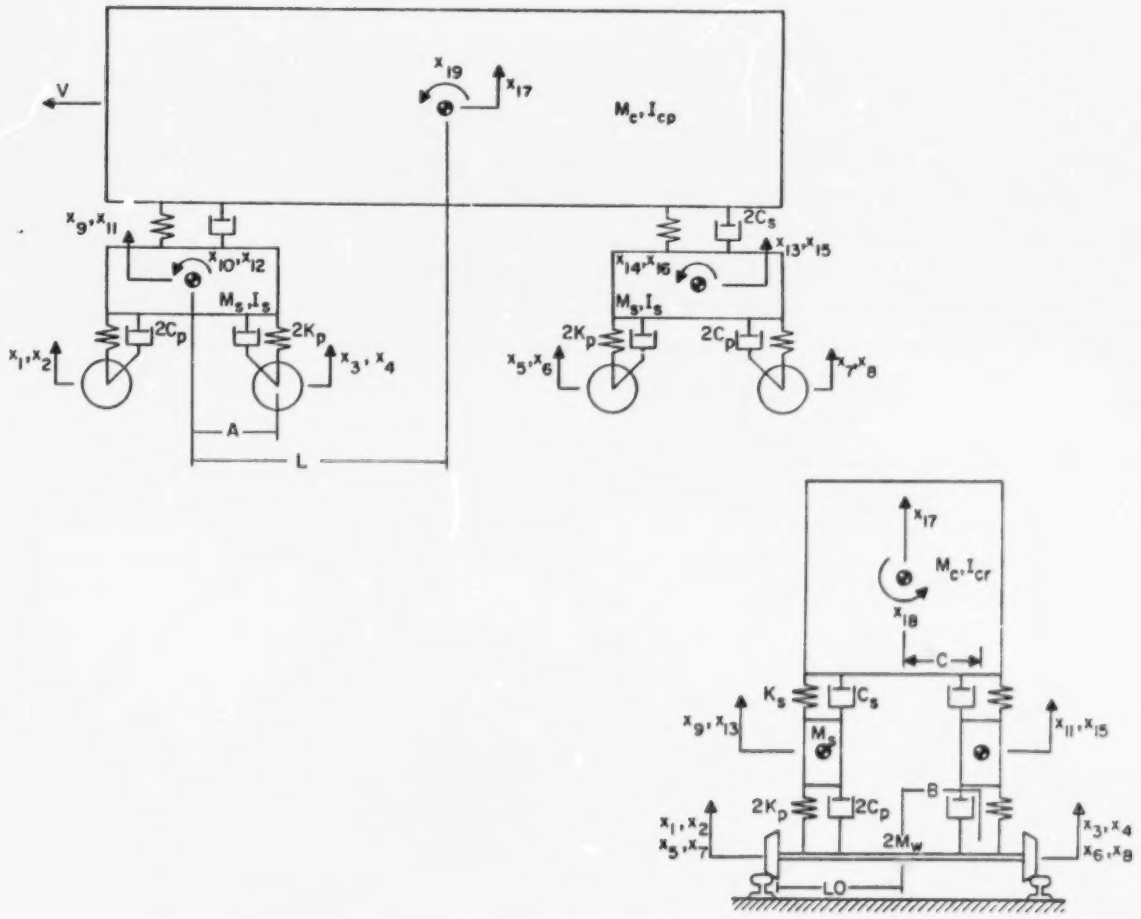

Figure A.2 Vertical vehicle dynamic model

The model is a simplified representation of any four-axle vehicle such as a 100-ton car, a four-axle locomotive, etc. It has 19 degrees of freedom:

(a)	wheel heave (8)	$x_1, \ldots x_8$
(b)	sideframe heave (4)	$x_9, x_{11}, x_{13}, x_{15}$
(c)	sideframe pitch (4)	$x_{10}, x_{12}, x_{14}, x_{16}$
(d)	carbody heave	x_{17}
(e)	carbody pitch	x_{19}
(f)	carbody roll	x_{18}

Each wheelset is connected to the sideframes by a primary spring and damper. Each sideframe is connected to the carbody by a secondary spring and damper. If the model is to be applied to another vehicle for which any of these springs or dampers do not exist, their value can be appropriately adjusted.

This model considers three basic assumptions. First, all mass components (namely sideframes, carbody, wheelsets) are assumed to be rigid. Second, all wheelsets are assumed to always be in contact with the rails. Third, all springs and dampers behave linearly.

A.4.2 Vehicle Input Data

A complete list of vehicle data required for vertical dynamic response simulation is given below. The masses, springs and dampers are labeled in Figure A.2.

A_1	=	half axle spacing
B	=	half distance between primary suspension elements
C_o	=	half distance between secondary suspension elements
L_o	=	half distance between wheels
L	=	distance carbody centre-of-gravity to secondary suspension
M_{ax}	=	mass of wheel and half-axle
M_{sf}	=	mass of sideframe
M_{bod}	=	mass of carbody
I_{sf}	=	sideframe inertia
I_{rot}	=	carbody rotational inertia
I_{pt}	=	carbody pitch inertia
K_1, K_2	=	primary, secondary spring stiffness
C_1, C_2	=	primary, secondary damping coefficients

These input data are stored in computer files which are read by the main program during the simulation runs. Dynamic simulations may be made for any four-axle vehicle operating at any speed by creating a data file with the corresponding parameters. Heavy and light freight cars, passenger coaches and four-axle locomotives can all be represented by this model. A sample data set representing a 100-ton hopper car is shown below.

A_1	= 0.9 m	I_{sf}	= 1.1×10^5 kg/m^2
B	= 1.003 m	I_{rot}	= 3.6×10^4 kg/m^2
C_o	= 1.003 m	I_{pt}	= 1.8×10^6 kg/m^2
L_o	= 0.7176 m	K_1	= 2.827×10^7 N/m
L	= 5.5 m	K_2	= 3.88×10^6 N/m
M_{ax}	= 7.1×10^2 kg	C_1	= 6.2×10^4 Ns/m
M_{sf}	= 7.3×10^2 kg	C_2	= 1.11×10^5 Ns/m
M_{bod}	= 4.5×10^2 kg		

A.5 TRACK CHARACTERIZATION

The Track Index Program calculates the following characteristics for each sample section of digitized track geometry errors:

- standard deviation (amplitude indication)
- frequency index (an indication of the predominant wave length)
- CN track geometry index (an indication of the product of frequency and amplitude).

The CN index formula is:

$$I = \sum_{i=1}^{n} \frac{| y_{i+1} - y_i | * 10^5}{L}$$

where: I = track index

L = track section length (m)

y_i = track deviation at point i.

n = number of points over L metres of track

Track surface and cross-level indices are calculated over 50 m sample lengths for 50 m simulation runs, and over 30 m sample lengths for 30 m simulation runs.

A.6 SIMULATION RUNS

Over 100 simulation runs were made with the Vertical Dynamic Model simulating a 100-ton hopper car running at speeds of 5-33 m/s (10-75 mph) over a variety of track sections. Vehicle dynamic force variance (i.e. standard deviation of dynamic force) was determined for various vehicle speeds and track SI/CI.

A.7 EMPIRICAL EQUATION

An empirical equation expressing vehicle dynamic force variation as a function of vehicle speed and track indices as derived from simulation results is shown below.

$$\delta = 10^{-3}\, V^{.68}\, (.585\, SI^{1.4} + 1.22\, CI)$$

where: δ = one standard deviation of dynamic force variation (kN)

V = vehicle speed (m/s)

SI = Surface Index

CI = Cross-level Index

The correlation between this equation and simulation results is shown in Figure A.3.

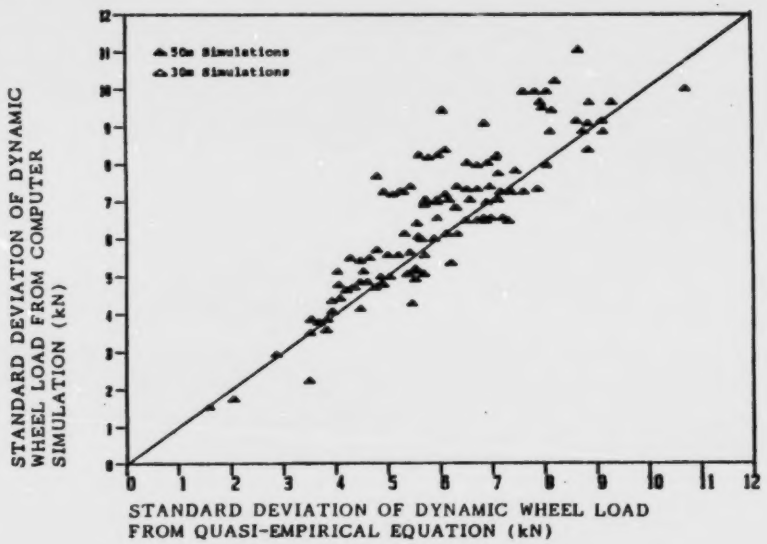

Figure A.3 Correlation between simulated and calculated values of the standard deviation of dynamic wheel load

For general application, the above equation can be generalized to provide a dynamic load factor as follows:

$$\phi_d = \frac{\delta}{145} \times (.44)^{.68}$$

$$= 3.97\ E\text{-}6\ V^{0.68}\ (0.585\ SI^{1.4} + 1.22\ CI)$$

where 145 is the nominal wheel load (in kN) of the 100-ton car and (.44) is the conversion factor for vehicle speed, V, in mph.

A.8 VALIDATION

A.8.1 Dynamic Force Increment as a Function of Speed

(a) Battelle-Columbus Data

The effect of speed (i.e. the power .68) in the empirical equation agrees well with U.S. field data for 100-ton cars (i.e. the power .66) shown in Figure A.4.

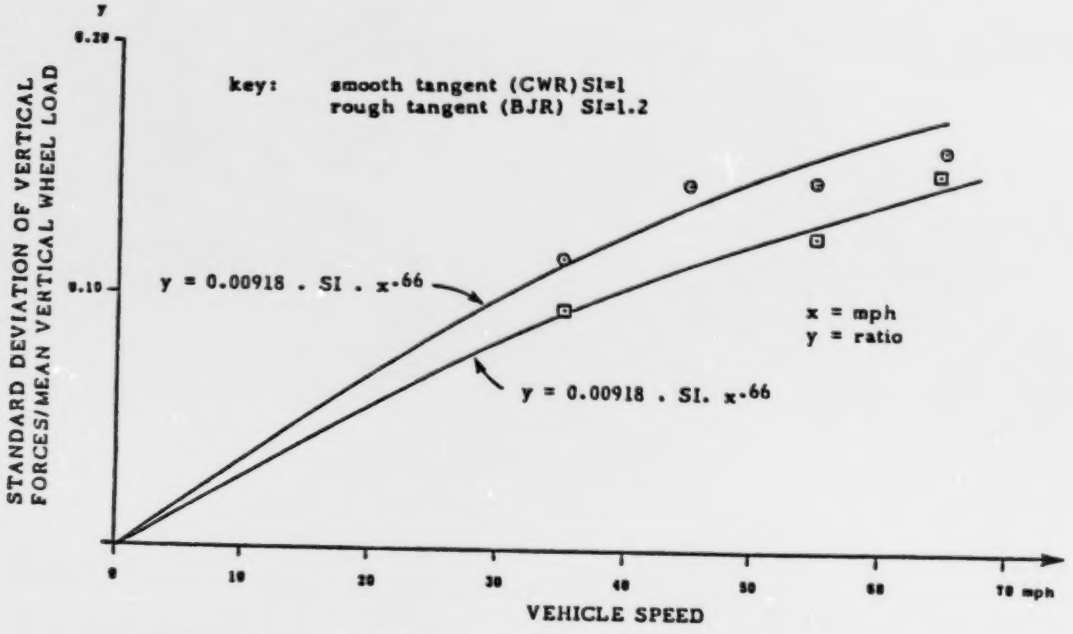

Figure A.4 Effect of speed on dynamic wheel load for a 100-ton car (Alhbeck)

(b) Canadian Railway Data

The effect of speed ($V^{.68}$) is further substantiated by field data collected on a Canadian railway subdivision work train test. Impact loads were measured at five strain gauge locations for wheels with and without defects. Test speeds were from 2.3 to 55.2 mph. Test data from 13 normal wheels (no defects) are used for this validation.

Data Analysis:

- mean dynamic load was determined for each wheel at each speed from five strain gauge readings
- measured loads at 2.3 mph were consistently higher than at 5.4 mph. Data at 2.3 mph were discarded and measured loads at 5.4 mph were considered steady state vertical load
- dynamic increment was calculated for each wheel at each speed as:

$$\sigma_{vi} = Fd_{vi} - Fd_o$$

where: σ_{vi} = dynamic increment at speed (vi)

Fd_{vi} = mean dynamic load at speed (vi)

Fd_o = mean steady-state load.

The data obtained were plotted against a family of curves of the form:

$$\sigma = a\ V^{.68}$$

where: σ = dynamic increment (kips)

a = constant representing wheel characteristics.

Except for two wheels, (4B and 12A), the data generally indicate that the effect of speed can be reasonably represented by a power of 0.68 (i.e., $V^{0.68}$). Two sample results are shown in Figures A.5 and A.6.

A.8.2 Calibration

Unfortunately, Canadian railway data are not appropriate for direct comparison with the calculated dynamic load factor. Due to the fixed

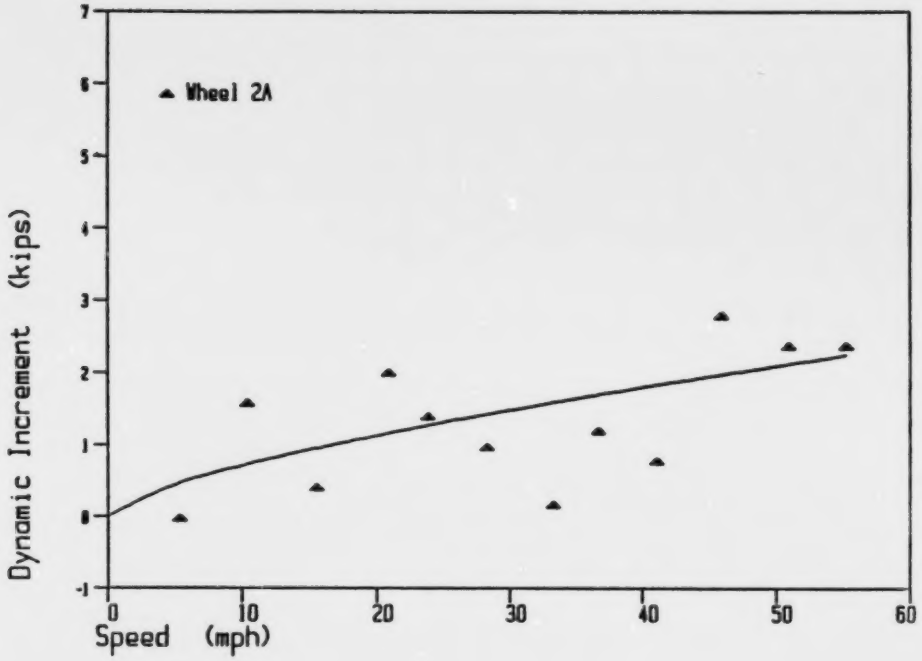

Figure A.5 Dynamic wheel load increment versus speed - Wheel 2A

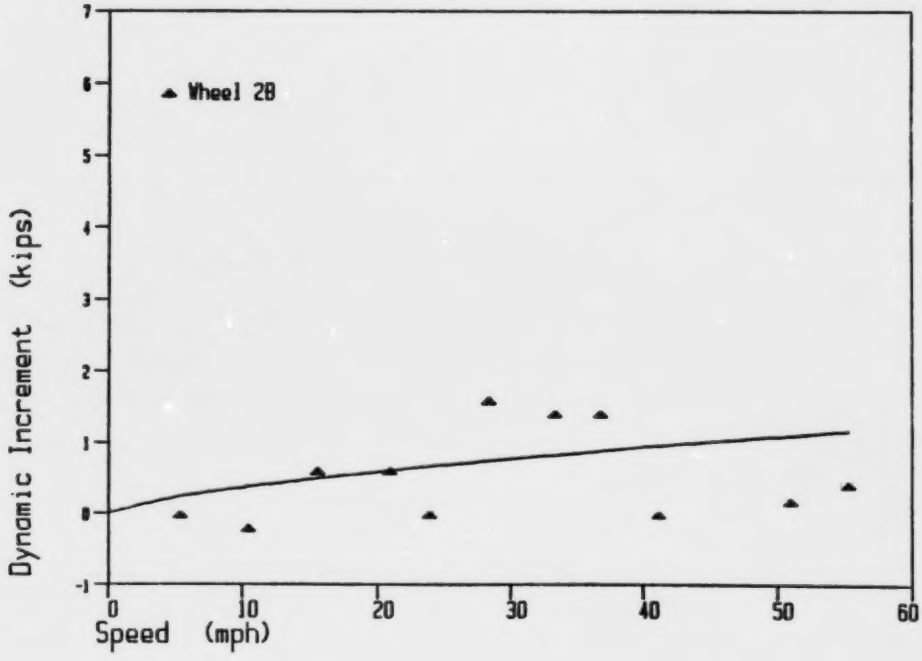

Figure A.6 Dynamic wheel load increment versus speed - Wheel 2B

location of the strain gauge system in track, the response to dynamic wheel load to track geometry error (i.e. different values for surface and cross-level indices) could not be measured. The Battelle-Columbus data show that the dynamic load factor for CWR and BJR track varies in the range of 0.10 to 0.15, depending on vehicle speed (range 35 to 65 mph). This is roughly twice the dynamic load factor obtained through computer simulation. The discrepancy is likely due to the fact that the track geometry data used in the simulation (obtained by the track recorded car) did not contain short-wave (high-frequency) error information. Until this matter is adequately resolved, a factor of 2 will be used to bring the calculated dynamic load factor to the same range as the Battelle-Columbus data. The dynamic load factor is thus given by:

$$O_d = 7.94\ E\text{-}6\ V^{0.68}\ (0.585\ SI^{1.4} + 1.22\ CI)$$

A.9 DYNAMIC FORCE ESTIMATION FOR OTHER VEHICLES

The empirical equation expressing the dynamic force variation of a 100-ton car to vehicle speed and track indices is expanded to express the dynamic force variation of other vehicles. Of interest are locomotives, passenger coaches, and 50-70 ton freight cars.

Theoretically, each vehicle has its own set of eigen-frequencies which characterize its unique dynamic response to track roughness. Therefore, each type of car must be given a full analysis as was done for the 100-ton car. The lack of data on vehicle parameters for most vehicles (except the 100-ton car), plus the complexity of the analysis, make this option impractical for the present project.

As an approximation, the quasi-empirical equation developed for the 100-ton car is adapted for other cars using a relative unsprung mass term, as follows:

$$P_d = 7.94\ E\text{-}6\ P_s\ V^{0.68}\ (0.585\ SI^{1.4} + 1.22\ CI)\ (M_u/3156)^{0.5}$$

where: Pd = one standard deviation of the dynamic wheel force variation (lbs)

P_s = steady-state wheel load (lbs)

V = vehicle speed (mph)

SI = surface index

CI = cross-level index

$\frac{M_u}{3156}$ = ratio of vehicle unsprung mass to that of a 100-ton car.

Research into vehicle dynamics has identified unsprung mass as the most significant vehicle parameter to dynamic wheel force increment at high speed. The adaptation, therefore, is considered a reasonable estimate for the present.

APPENDIX B

RAIL COST MODEL

B.1 OUTLINE

This program provides a method for attributing a share of rail costs to individual train traffic based on current knowledge of wheel/rail interaction and material behaviour.

Figure B.1 describes the conceptual approach. It basically shows that rail damage and associated costs are caused by an accumulation of various wheel loading cycles, each with a different dynamic force, depending on vehicle characteristics, operating conditions, and track quality.

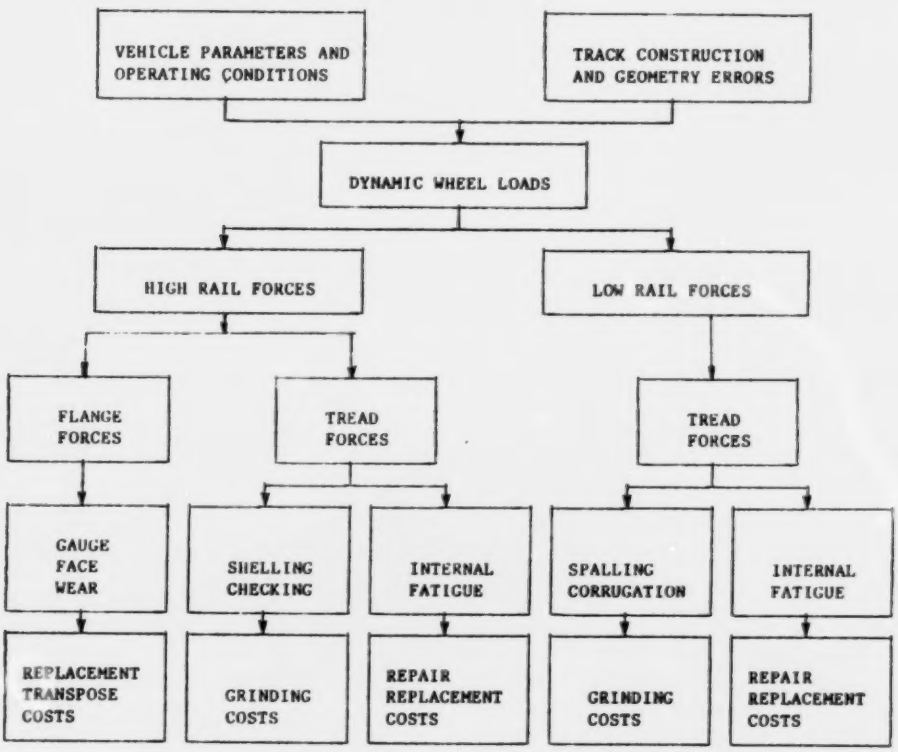

Figure B.1 Concept of rail cost model

Generally, if the total cost is known and the accumulated wheel load cycles can be normalized so that each "equivalent cycle" causes equal amounts of damage, then a unit of rail cost per cycle can be established, e.g.:

UNIT COST = TOTAL COST/TOTAL EQUIVALENT CYCLE

If a traffic category such as "passenger train" causes Np equivalent cycles, its share of the rail cost will be:

PASSENGER COST = UNIT COST * Np

The key to this approach is to accurately estimate the dynamic force exerted on the rail by each traffic category, and the relative extent of damage the rail sustains when subjected to a cycle of such force. This is explained in more detail in the following section.

B.2 WORKING EQUATIONS

B.2.1 Estimation of Wheel Forces

The static wheel force, Po, is derived from the average loaded vehicle weight. The steady-state force, Ps, is calculated as the load transfer due to unbalanced curving speed. Superelevation is assumed set for 60 mph freight speed.

The dynamic force is calculated with a quasi-empirical equation the of standard deviation of dynamic force fluctuation versus speed. The equation is developed using a full-body dynamic model of a 100-ton car.

$$\sigma = 7.94 \times 10^{-6} * V^{.68} * (.585 * SI^{1.4} + 1.22 * CI)$$

where: σ = standard deviation of dynamic force

V = vehicle speed

SI = track surface index

CI = track crosslevel index

The steady-state lateral tread force is estimated as the average lateral force created by the leading wheelset on high and low rails. Flange force is twice that.

$$F = (P/35000)^{2/3} * (9.6\ D^{.552} + 1)$$

where: F = steady-state lateral wheel load (lb)

P = static wheel load (lb)

D = degree curve.

These force estimations are documented in Appendix A and will be subject to further refinement in the near future.

B.2.2 Estimation of Rail Wear and Fatigue

The rate of gauge face wear on the high rail is proportional to the flange force and friction factor.

$$Ne = N * (F_f * \mu_a / F_{ref} * \mu_{ref})$$

where: Ne = equivalent cycles

N = cycles

F_f = flange force

μ_a = friction factor (actual)

F_{ref} = reference force

μ_{ref} = reference friction factor.

The rate of fatigue damage is dependent on the maximum range of octahedral shear stress created by a passage of each wheel.

$$Ne = N * (Soa/So_{ref})^{3.5}$$

where: Soa = octahedral stress (actual)

So_{ref} = reference octahedral stress.

A power of 3.5 corresponds to the crack propagation mode. The octahedral shear stress ranges from 0.30 po for tread force equals zero, to 0.63 for tread force equals 1/3 of vertical force. po is the maximum contact stress at the surface. It is given by:

$$po = 23452 * Sum\ (1/R)^{2/3} * P^{1/3}$$

where: po = maximum contact stress at surface

Sum(1/R) = sum of longitudinal and transverse radii for wheel and rail

P = impact load.

On low rail, higher contact stress is expected for incidences of false flange contact. It is currently assumed that 10 per cent of freight wheels have false flanges and 50 per cent of curves have wide gauges, resulting in a false flange contact probability of 5 per cent. Passenger wheels are assumed to have no false flange. Maximum stress under the false flange contact condition can be calculated once data on false flange wheels become available. For now it is estimated to be twice the normal contact stress.

B.3 PROCEDURE TO ESTABLISH RAIL COST DATA

B.3.1 Curved Rail Replacement Cost Breakdown

The following actions and assumptions establish rail cost data:

- survey the location where rails are soon to be replaced
- measure side wear and head wear
- assume that side wear is the main cause for replacement
- assume that transposition of rail is normally carried out
- assume that the total side wear possible is the side wear limit specified in SPC

- call this "SWL" and call the measured side wear "SW."

The proportion of rail replacement cost due to side wear is:

$$Ks = SW/SWL$$

The remainder of the rail replacement cost is due to surface defects such as shelling, corrugation, etc. Note that the rail replacement cost discussed here (called "R$net") excludes rail replacement due to a high level of internal fatigue defects (called "R$if") and the rail change-out for up-grading the track (called "R$up"). Assume that rails are not relaid elsewhere (however, if this is the case an adjusted rail cost must be applied). The total rail replacement cost shown on the subdivision budget is made up as follows:

$$R\$gross = R\$net + R\$if + R\$up$$

This can be further brakedown as follows:

$$R\$net = R\$sw + R\$sfH = R\$sfL$$

where: R$sw = cost of rail side wear

T$sfH = cost of surface defects on high rail

R$sfL = cost of surface defects on low rail

and

$$R\$if = R\$ifH + R\$ifL$$

where: R$ifH = cost of internal rail fatigue on high rail

R$ifL = cost of internal rail fatigue on low rail

R$ifH and R$ifL can be determined using records of rail flaw distribution (i.e. per cent on high rail, per cent on low rail) and special rail supply requests due to rail fatigue defects (e.g. miles of rail that must be replaced because the fatigue rate has reached two defects/mile/year) can be made.

R$sfH and R$sfL can be determined using the rail grinding record to be discussed in detail later. For now, let us call mgH the total miles of grinding because of high rail surface problems, and mgL that for low rail. Assuming regular grinding is sufficient to keep the rail surface in acceptable operating condition (that is, rail surface problems result in rail replacement need via rail head loss due to grinding), the following relationship can be established:

$$R\$sfH = R\$net * (1-Ks) * (mgH/(mgH + mgL))$$

$$R\$sfL = R\$net * (1-Ks) * (mgL/(mgH + mgL))$$

B.3.2 Curve Rail Maintenance Cost Breakdown

Rail maintenance cost is made up of:

- internal fatigue defect repair (e.g. plugging) cost (indirect costs such as train delays, derailment, etc., may be included)
- surface defect repair (e.g. grinding) cost.

The breakdown of total rail internal defect costs to high and low rail can be made using instrumented car data.

The breakdown of total rail grinding costs to high and low rail can be made by surveying locations where grinding is required. For each curve one can establish a reason for grinding based on rail surface conditions. For example:

- curve #1: 0.3 miles of grinding needed; shelling on high rail
- curve #2: 0.25 miles of grinding needed; shelling on high rail and corrugation on low rail (50/50)

From these records the total miles of grinding due to high and low rail, mgH and mgL, respectively, can be calculated.

Each component of rail maintenance cost can be added to the respective component of rail replacement cost to derive the following final cost data for use in the "Rail Cost Distribution Model":

- cost of side wear on high rail
- cost of fatigue on high rail
- cost of fatigue on low rail.

Note that for tangent track internal fatigue defects are usually the only problem.

APPENDIX C

SURFACING MAINTENANCE COST MODEL

C.1 INTRODUCTION

The objective of this project is to develop a computer model which relates the cost of track surfacing/maintenance to traffic. Its purpose is to aid the railroad manager in the systematic analysis of track maintenance cost and the optimization of track maintenance planning. Examples of topics of current interest are:

- determining the cost contribution by a specific traffic category in an existing traffic mix
- determining the optimal trade-off between manual surfacing gang capacity and the mechanized surfacing cycle.

Construction of the model will be based on existing scientific knowledge of vehicle/track interaction and track support behaviour. Wherever such knowledge is unavailable, engineering judgments will be made. The intention is to complete the model with the proper structure and elements of the best possible quality.

Trial applications of the model to actual railroad operating environments will test its versatility and suitability. Critical evaluation of the model by track researchers based on their ongoing work will help upgrade its scientific validity.

Thus, the basic goal of this work is to produce an immediate tool for railroad managers and a focus for track researchers.

C.2 GENERAL PLAN

The relationship between surfacing cost and traffic can be established in two stages:

- surfacing cost as a function of track geometry error
- track error as a function of traffic.

The main task in the first stage is to identify a quantifiable parameter which represents track geometry quality and can be used as a criterion for planning surfacing work.

The main task in the second stage is to identify the mechanism which links traffic to track error growth. Both "traffic" and "track error" must be represented by quantifiable parameters. The identified mechanism can then be used to normalize the wheel load cycles of different traffic categories to a standard load. A traffic mix is thus reduced to an equivalent uniform traffic whose loading can be directly compared against the actual data on track geometry error growth to form an empirical relationship.

C.3 RELATIONSHIP BETWEEN SURFACING CYCLE AND TRACK GEOMETRY ERROR

C.3.1 Concept

The principal method of correcting track surfacing error is tamping. It is routinely carried out by manual work gangs. Periodically, when track error is beyond the capacity of the local work gangs, mechanized equipment is provided by the region for a systematic reconditioning of track geometry. This is known as a surfacing cycle. Since ballast also degrades under traffic, a small amount of ballast is added at each surfacing cycle to compensate for the degradation. This is known as lifting.

The basic criteria for surfacing work on North American railroads are maximum allowable track geometry error limits. These are set for safety reasons and, because they are listed in the Standard Practice Circular, are known as SPC limits. Normally, the magnitude of track errors increases under traffic but their position (i.e. spatial distribution) is unchanged. Consequently, the manual tamping work usually involves inspecting and correcting the usual problem sites.

The relationship between mechanized and manual surfacing work can be described mathematically by considering the track as a long chain of individual elements (see Figure C.1). Each element would deviate from the ideal geometry by a certain amount called error. Most elements have errors below the safety limit and make up the "good" portion of

track. A few have errors above the safety limit and must be corrected. These make up the "poor" portion of track. Note that "poor" track is not fully condemnable. Typically, the length of a track error element is 39 feet (i.e. original rail length). A condemnable error at each rail length requires tamping (manual) approximately three times (about 5 feet). This is only about 13 per cent of the rail length. Thus, for each mile of "poor" track only .13 miles need repair.

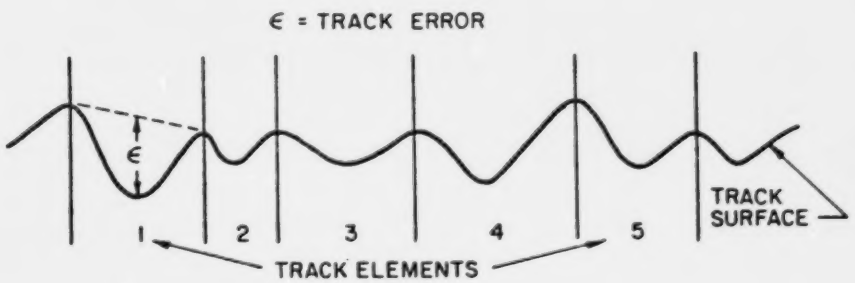

Figure C.1 Idealized representation of track geometry errors

Assuming that track errors are normally distributed with a mean, x, and standard deviation, s, the relationship between track condition and work load is as follows:

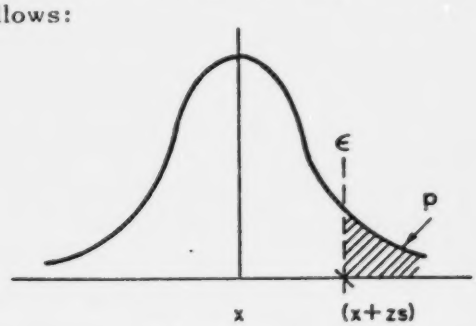

TRACK ERROR DISTRIBUTION

p = per cent of "poor" track

$$= f(z) = \int_{-\infty}^{x} \frac{1}{\sqrt{2\pi}} \ell^{-u^2/2} \, du$$

where: $z = (-x)/s$

= safety limit

The distribution of track error can be readily established using a track recording car. From this, the per cent of poor track can be calculated for a given set of safety limit criteria.

"Per cent of poor track" is a relevant parameter representing overall track geometry quality. It is implicitly used in the current process of surfacing planning on North American railroads. Figure C.2 summarizes this concept

C.3.2 Mathematical Model

Different railroads may use different sets of maximum allowable track geometry error limits. Some are based on safety; others include economic considerations. A universal formula therefore is not possible. The procedure for establishing "per cent of poor track," however, is common to all and can be illustrated through an example case which is quite common in North America.

DESCRIPTION

Track A consists of 500 miles of mainline double track carrying a mix of light and heavy freight traffic and high speed passenger traffic. The SPC states the following safety limits:

- surface error $\leq$ 0.5 inch
- cross-level error $\leq$ 1 inch

Other errors are less relevant and hence not cited here.

Errors can be measured manually using a 62-foot chord. The principal method of track geometry inspection, however, is by track recording car. This car measures track geometry error under its dynamic load.

The weight of the car alone is known to compress the track slightly, resulting in a dynamic error measurement slightly larger than a static measurement. Moreover, the error data is provided as peak-to-trough distance, irrespective of the 62-foot chord. Figure C.3 is a sketch of typical data. A 62-foot chord is superimposed at one location to illustrate the SPC limit method.

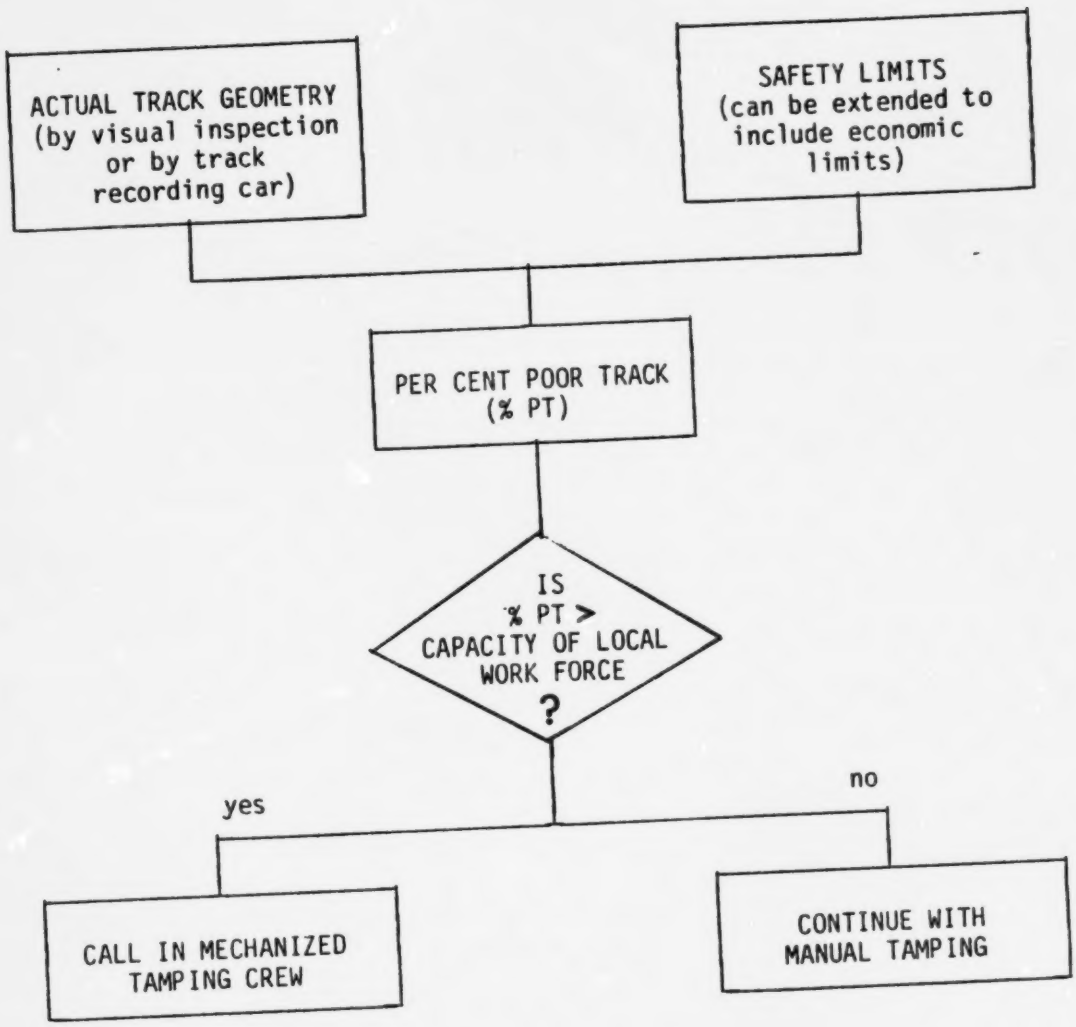
ACTUAL TRACK GEOMETRY (by visual inspection or by track recording car)
SAFETY LIMITS (can be extended to include economic limits)
PER CENT POOR TRACK (% PT)
IS % PT > CAPACITY OF LOCAL WORK FORCE ?
yes
no
CALL IN MECHANIZED TAMPING CREW
CONTINUE WITH MANUAL TAMPING

Figure C.2 "Per cent poor track" as a criterion for mechanized tamping cycle

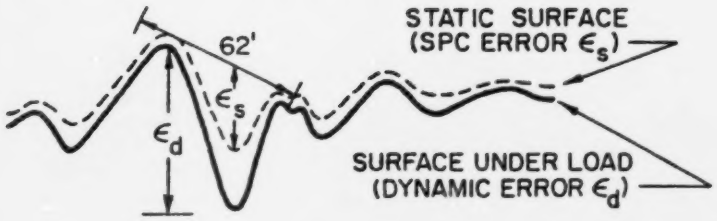

Figure C.3 Track geometry error and methods of measurement

It can be seen that if a 62-foot chord is used to measure error (ϵ), it may be either larger or smaller than the peak-to-trough value, depending on the waveform. Currently there is no method of resolving the difference between the SPC (static) method and the recorder-car (dynamic) method. Local track maintenance personnel consequently set their own standard. They use the track recorder car data and treat left and right rails separately. Only one error limit is used:

$\epsilon \leq$ 0.5" peak-to-trough error for either rail

The distinction between surface and cross-level error is thus removed, as is the difference between static and dynamic measurements. Experience has shown that this method meets the SPC limits (which are still the ultimate standards) and produces high track quality.

PER CENT POOR TRACK

One-third of the track is tamped each year, resulting in a surfacing cycle of three years. The work can be idealized as mechanically tamping continuously from one end of the track to the other, taking three years to complete the cycle. The overall track quality, therefore does not change, since the rate of track error growth is balanced against the surfacing capacity (manual plus mechanized). Therefore, any track recording run is representative, in theory, of the steady-state track quality. In practice, the mid-summer run is most representative, considering the local climate, and hence is selected for this analysis.

An analog record of the track geometry car data in July 1985 is first digitized to obtain a track error measurement every 2 feet. The result is then processed to give the mean (x) and standard deviation (s) of track error (peak-to-trough) in each unit of 0.05 miles of track (left

and right rails are treated individually). The 0.05 miles unit length was selected for ease of analysis and to allow for detailed sectioning of track with negligible position error.

From the work record of the mechanized tamping unit, the whole track length is broken into sections and grouped according to the year since it was last tamped. The following groups are created:

1985 - just tamped (within a month)
1984 - one year since last tamping
1983 - two years since last tamping
1982 - three years since last tamping.

The result is:

Year	Years Since Tamping	Mean Error	Standard Deviation of Error
1985	0	.247"	.140"
1984	1	.271"	.150"
1983	2	.294"	.160"
1982	3	.315"	.170"

The corresponding estimate of per cent poor track is (assuming normal distribution and an error limit of 0.5 inch):

Years Since Tamping	z	p(%)
0	1.81	3.5
1	1.53	6.3
2	1.29	9.85
3	1.09	13.8

Based on the foregoing idealization of track tamping work, the above results can be interpreted as follows:

- 1/3 of track has from 3.5 to 6.3 per cent poor track
- 1/3 of track has from 6.3 to 9.85 per cent poor track
- remaining track has from 9.85 to 13.8 per cent poor track.

The overall average per cent poor track is therefore:

$$p = \frac{1}{3}\left(\frac{3.5}{2} + 6.3 + 9.85 + \frac{13.8}{2}\right)$$

$$= 8.3\%$$

The length of poor track out of a total of 500 miles is:

$$\ell = 500 \times 0.083$$

$$= 41.5 \text{ miles}$$

Eight point three per cent and 41.5 miles are two parameters representing the current track quality and work load, respectively.

4. RELATIONSHIP BETWEEN TRACK GEOMETRY ERROR AND TRAFFIC

4.1 Concept

If traffic is uniform (e.g. all unit trains), the relationship between track geometry error growth and wheel loading cycle can be empirically determined using a regression technique on actual data.

If, however, traffic is not uniform, the actual wheel loading cycle must first be normalized. The normalization converts the actual wheel cycles into the equivalent cycles of a reference traffic. The normalization must be based on the relative significance of different wheel loads on track geometry degradation. The reference wheel load should be from the main traffic type in a traffic mix.

This process of model development stays close to actual experience and only depends on the relative significance of some key variables in the track degradation phenomenon. It is designed to produce reliable results using the current incomplete understanding of track behaviour.

In the following, the current understanding of track degradation under traffic will be described and a corresponding procedure for normalization of wheel loading cycle will be presented.

4.2 Outline of Track Geometry Degradation Process

Research to date on track geometry degradation has indicated that under traffic the amplitude of track errors grows but their positions (i.e. spatial distribution) remain basically unchanged (see Figure C.4). Therefore, the growth of track error amplitude is proportional to the rate of differential track settlement.

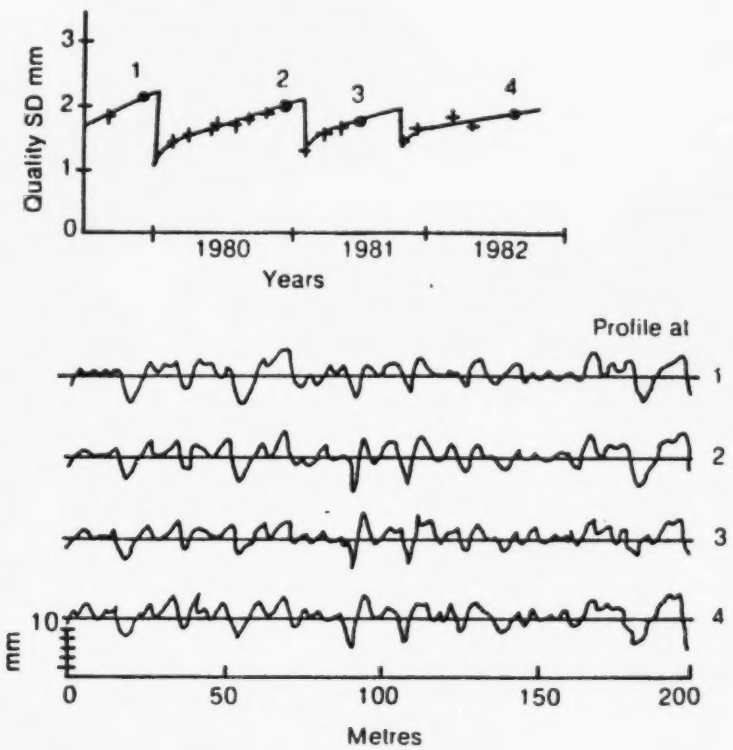

Figure C.4 The vertical profiles of a section of track towards the end of four maintenance cycles (ref. Shenton, 1984)

For a given track error location, the trough area received maximum dynamic load (nominal load + dynamic increment), while the peak area received minimum dynamic load (nominal load - dynamic increment). This happens under each wheel load of the total traffic mix.

The trough area, therefore, settles faster than the peak area, resulting in a differential settlement rate which increases track error amplitude. Figure C.5 schematically described this process.

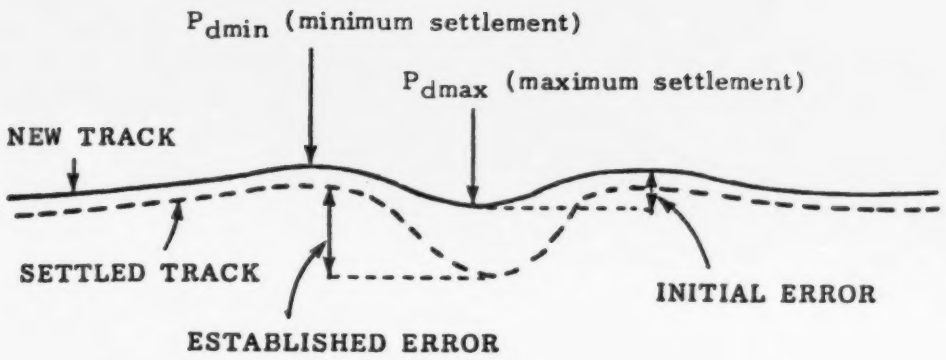

Figure C.5 Track differential settlement and error growth

Given a wheel load, the settlement rate is a function of the following factors:

- number of loading cycles
- stress exerted on the ballast
- compressibility of the subgrade
- ballast quality.

Details of the factors are given in the following sections.

C.4.3 Effect of Stress on Ballast

For any given track design, different wheel loads create different stresses on the track bed, resulting in different track settlement rates. CN test data (see Figures C.6 and C.7) shows that most track settlement occurs within the ballast/subballast layer. This is expected to be generally true for track which is properly designed and maintained.

Various laboratory studies of ballast settlement, from small-scale tri axial tests to large scale ballast box tests, have indicated a general trend to permanent track settlement increasing with applied stress on the ballast. The relationship is not well defined due to the complexity of the ballast system. Based on a survey conducted by Selig and Alva-Hurtado (1982), it can be generally concluded that track settlement after a given number of cycles is proportional to ballast stress raised to a power of 1 to 3. A power of 1 is likely for strong ballast

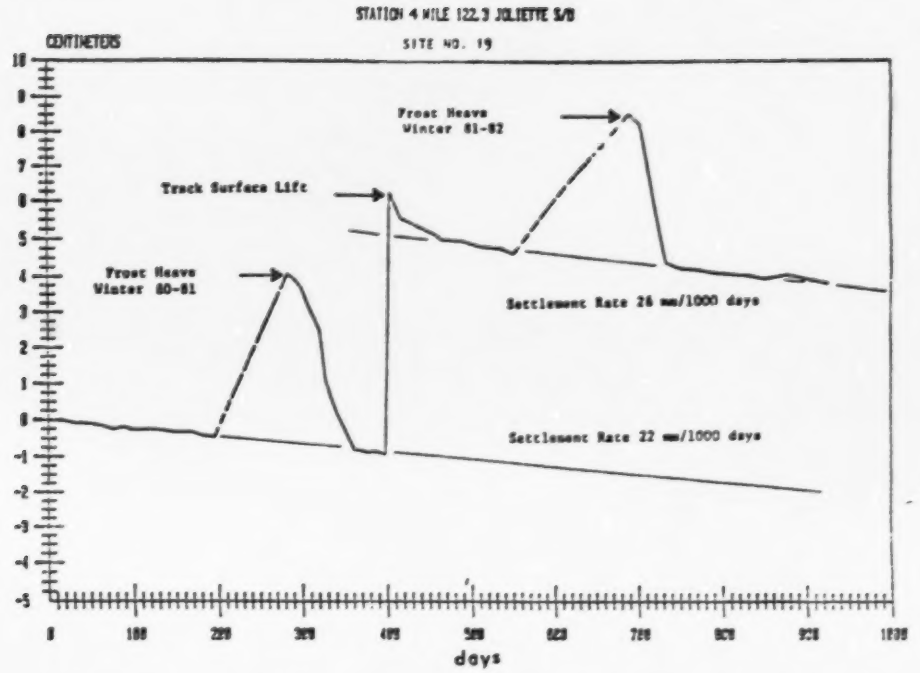

Figure C.6 Total track settlement measured at rail level

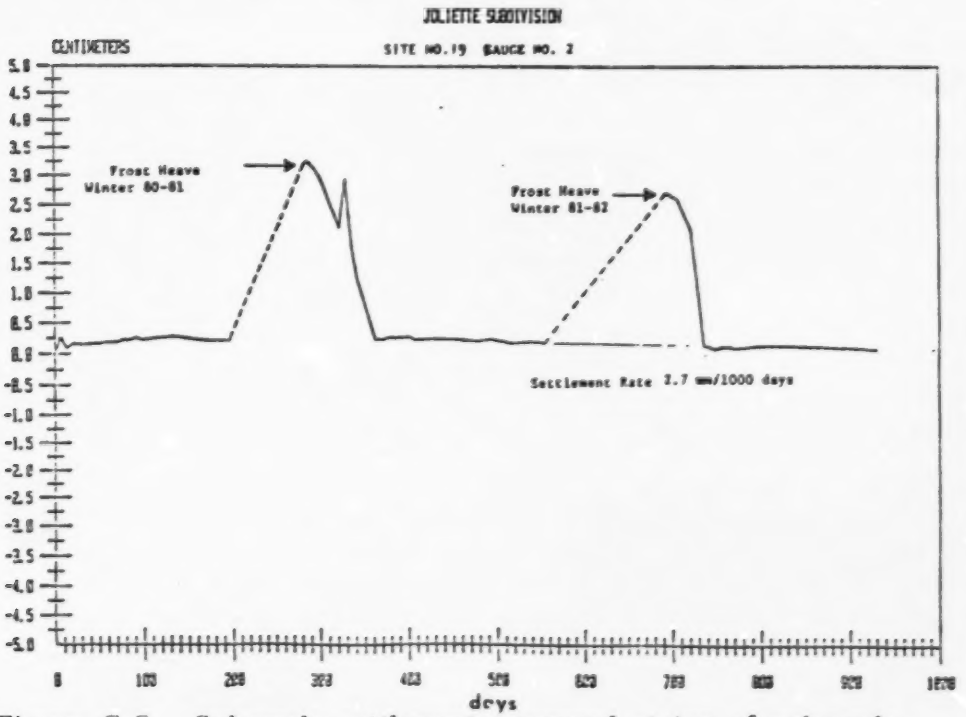

Figure C.7 Subgrade settlement measured at top of subgrade, 20" below base of tie

subjected to relatively light loads; and a power of 3 is likely for weak ballast subjected to relatively heavy loads. Figure C.8 is an example of laboratory data on ballast settlement.

Raymond(1985) in a recent study of track settlement using a large-scale ballast box (Figure C.9), found that track settlement after a given tonnage was proportional to applied load raised to a power of 1 for loads less than threshold and up to 3 for loads greater than threshold. Threshold load is defined as the load level beyond which large track settlement occurs. Since doubling the wheel load results in achieving the same tonnage at half the number of cycles, the above relationship indicates that for a given number of wheel loading cycles, the track settlement rate is more than proportional to ballast stress.

The relationship between track settlement and ballast stress still requires further investigation, especially for typical North American track conditions. For the time being, it may be estimated from the above research findings that track settlement rate is proportional to the square of ballast stress.

C.4.4 Effect of Load Cycle Accumulation

Data on actual track settlement on CN track, recorded in a four-year test program by the CN Rail Research Centre (Dalton and Scott, 1983) showed quite consistently that long-term permanent settlement of track increased linearly with time (ref. Figures C.6 and C.7).

The problem of frost heave during the winter months only affects the settlement rate temporarily. On average, track settlement during the frost heave period, which normally would include several freeze-thaw cycles and an extended period of frozen-solid, occurs at approximately the same rate as during the rest of the year.

The effects of a small surface lift (a few inches) are also temporary. There was a period of two to three months following the lift that the track settlement rate was high and decreased rapidly with time. Beyond this period, track settlement rate again became constant with time. Depending on the height of the lift and the subgrade condition, the new track settlement rate may increase slightly after a surface lift.

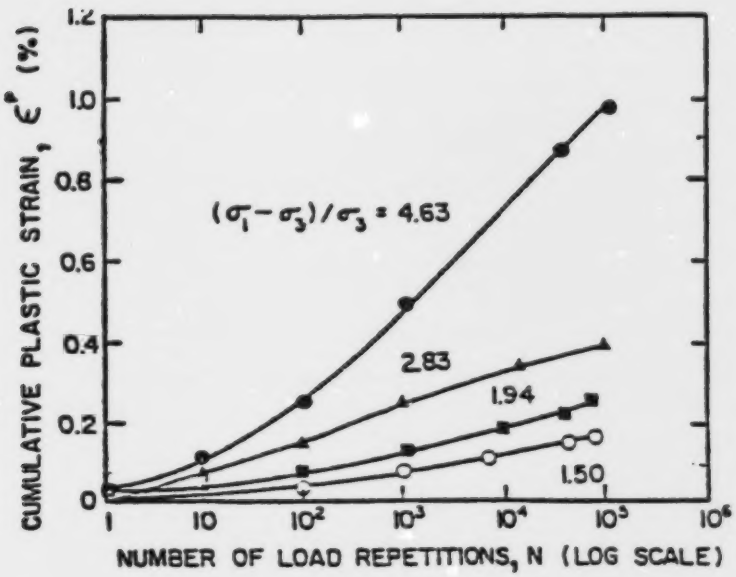

Figure C.8 Influence of number of load applications and magnitude of deviation stress on permanent deformation (ref. Barksdale, 1972)

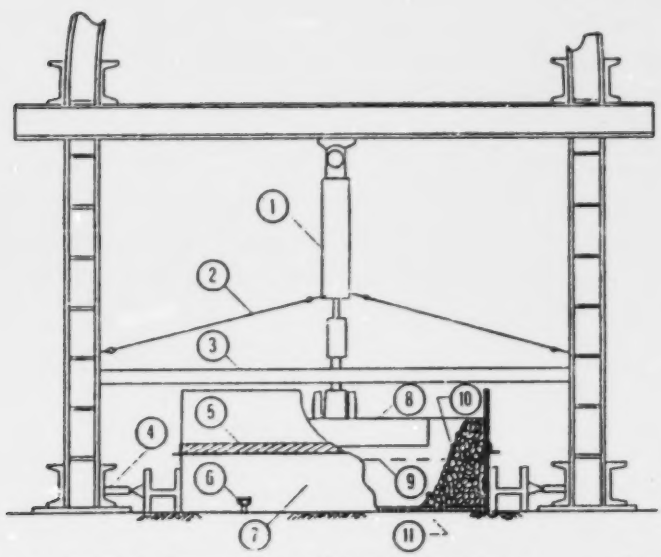

Figure C.9 Large-scale ballast-on-subgrade box test assembly (dimensions of box: 9' x 4.5' x 1.7') (Source: G.P. Raymond, 1985)

Data on traffic density indicates little change in annual tonnage during the test period. Assuming that the traffic mix also did not change much (e.g. no significant increase or decrease in the heavy-axle-load category), the time factor in track settlement measurements can be considered equivalent to the wheel load cycle. Thus, the following can be inferred from the CN test:

(a) long-term permanent track settlement increases linearly with the wheel-loading cycle

(b) frost heave and small surface lifting insignificantly affect the long-term track settlement rate.

It should be noted that most laboratory testings of ballast settlement (e.g. triaxial testing) show permanent settlement as a log function of load cycle (N) (re Figure C.8). The difference between laboratory test results (i.e. settlement $\propto$ log N) and field test results (i.e. settlement $\propto$ N) can be attributed to the fact that laboratory tests are mostly for short-term settlement of clean ballast. In practice, large surface lifts (e.g. during ballast undercutting and cleaning) rarely occur, while small surface lifts (e.g. during mechanized tamping) occur only infrequently (e.g. every few years). The log N relationship, therefore, is expected to be relevant only for the short period following a surface lift. For most of the remaining time of a surfacing cycle (from two to ten years), a linear relationship would prevail. For a practical analysis of track maintenance, the linear relationship will be used and the rapid settlement following a surface lift treated as part of the overall efficiency of the tamping process (i.e. an effective lift equals actual lift minus immediate settlement).

C.4.5 Effect of Ballast Quality

Ballast breakdown is one of the major contributors to track settlement. The effect can occur in two different ways. First, the broken-down ballast particles fill in the voids in the ballast layer, allowing further compaction and reduction of thickness (i.e. vertical settlement). Second, the abrasion of ballast particles creates fines which absorb moisture and act as a lubricant (re fouling). This allows ballast particles to move, resulting in track settlement. The presence of fines can also be caused by contamination from the top (e.g. air-borne dust) or bottom (e.g. subgrade pumping). Therefore, ballast quality is <u>not</u>

the only factor. Nevertheless, for well-maintained track, ballast quality can be considered the principal factor.

Laboratory test data produced from a comprehensive research program on ballast materials at Queen's University (1974-1982), indicated a strong correlation between ballast quality and plastic strain (i.e. settlement). Figure C.10 is a sample result showing different plastic strains for different grades of ballast materials. The correlation is apparent when the plastic settlement per $\log_{10}$ cycle is plotted against the aggregate index[1] as shown in Figure C.11. Data on the actual track maintenance cycle shown in Figure C.12 indicate the same general trend. Low-quality limestone and granite (I_a approximately 60) last less than 75 MGT between maintenance cycles; high-quality basalts and sulphide slag (I_a approximately 30) last up to 185 MGT between maintenance cycles.

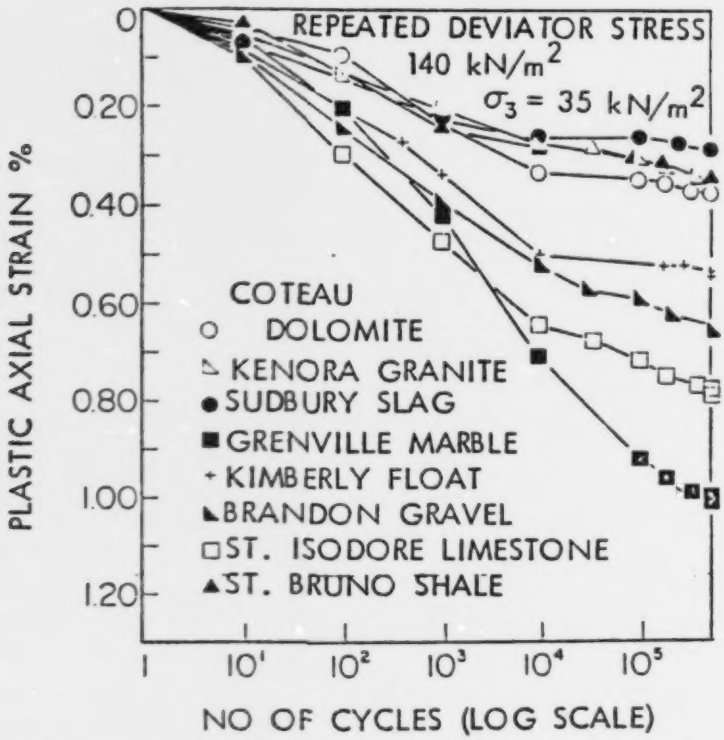

Figure C.10 Plastic axial strain observed in triaxial tests on railroad ballasts (ref. Raymond, 1979)

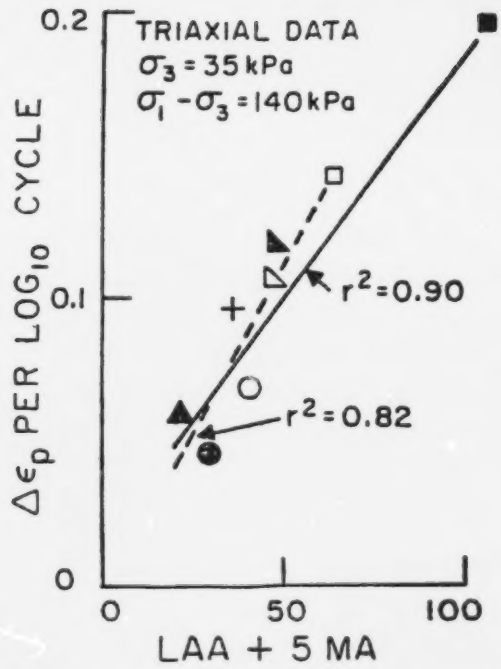

Figure C.11 Plastic strain per logarithmic cycle of loading versus aggregate index

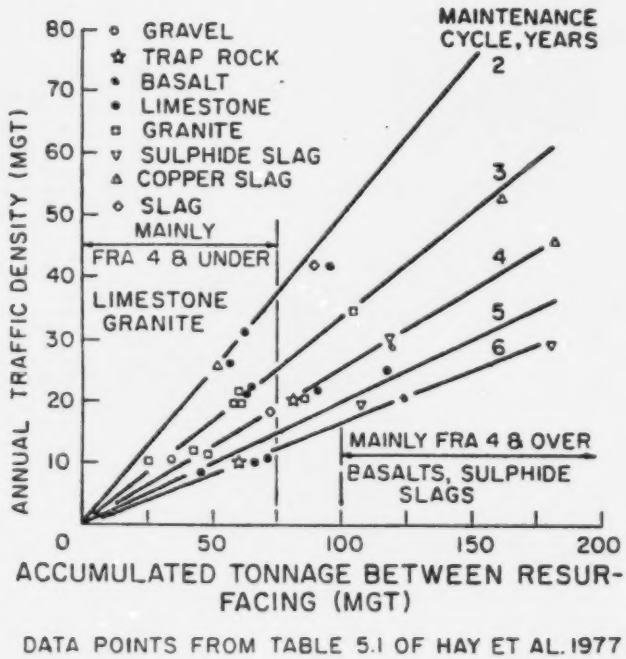

DATA POINTS FROM TABLE 5.1 OF HAY ET AL. 1977

Figure C.12 Mainline maintenance cycle related to aggregate index (ref. Raymond 1979)

The up-to-date research results outlined above indicate a relationship between ballast quality and track settlement rate, but do not provide sufficient data for a reliable quantification.

Further research is needed into the effect of particle shapes and the per cent of fines produced by ballast degradation. For the present it is assumed that the track settlement rate is proportional to the aggregate index (I_a).

C.4.6 Effect of Subgrade Compressiblity

It is a well-known fact that track built on a weak subgrade settles at a high rate. Preliminary laboratory tests at Queen's University (Raymond 1985) using a large-scale track section model with various types of subgrade material clearly indicated this trend.

In practice, areas of weak subgrade are given extra granular cover to reduce subgrade stress. The track section, if properly treated, would behave as if the subgrade is the same quality as nearby track built on stronger sugrade. Therefore, subgrade compressibility is not an appropriate parameter for use in actual track settlement studies. In addition, it is very impractical to characterize actual track with its subgrade compressiblity. Usually, track within a category is designed with the same standard, i.e. same rail and tie. Therefore, if there is any variation in the overall track stiffness (known as track modulus) it is due to the compressibility of the combined ballast/subgrade layer. If the ballast layer is constant (i.e. same aggregate and same thickness), the variation is due to subgrade (hence the problem is reduced to the laboratory test case).

Track modulus can therefore be used as a variable representing track support compressibility in the study of actual track settlement. This use is, however, correct only if rail and tie are the same (e.g. a change in track modulus due to the use of concrete ties may not relate to track settlement in the same way).

4.7 Combined Effect of Ballast Stress and Subgrade Compressibility

Both ballast stress and subgrade compressibility contribute to elastic track deflection. Using a beam-on-elastic model for track support and substituting wheel load and track modulus for ballast stress and sub-

grade compressibility, respectively, this relationship can be formulated as follows (Talbot, 1920):

$$y = \frac{P\lambda}{2U} \cdot \ell^{-\lambda x} (\cos \lambda x + \sin \lambda x)$$

$$\lambda = \left(\frac{U}{4EI}\right)^{1/4}$$

where: y = elastic track deflection (in.)

EI = rail section modulus (lb.in.^{2})

P = wheel load (lb)

U = track modulus (lb/in.^{2})

x = wheel position (in.)

The total elastic track deflection is the sum of deflection by each effecting wheel. Most of the deflection is due to the wheel right above the location ($x = 0$). Others can be the adjacent wheel on the same truck and the last wheel on adjacent car. For the current analysis, it would be adequate to assume that track elastic deflection is caused by three wheels, one at $x = 0$, and others 70 inches on either side. The total track deflection is therefore:

$$Y = \frac{P\lambda}{2U} (1 + 2\ell^{-70\lambda} (\cos 70\lambda + \sin 70\lambda)$$

Since ballast stress is proportional to wheel load, which in turn is proportional to elastic track deflection (see equation above), the previous assumption of track settlement being proportional to the square of ballast stress is equivalent to being proportional to the square of elastic track settlement.

This relationship indicates that:

- for the same track design, doubling the wheel load will increase the permanent track settlement rate four times
- for the same wheel load, halving the track modulus will increase the permanent track settlement rate by about 1.7 times.

C.4.8 Summary

The above analysis can be summarized as follows.

TRACK ERROR:

$$\epsilon \propto (S_{max} - S_{min})$$

where: ϵ = track error amplitude

S_{max} = track settlement under maximum dynamic wheel load (on trough area)

S_{min} = track settlement under minimum dynamic wheel load (on peak area)

TRACK SETTLEMENT:

Under uniform traffic, the track settlement is proportional to the number of loading cycles, i.e.:

$$S \propto N$$

The track settlement rate is proportional to the square of elastic track deflection:

$$S \propto \text{constant } Y^2$$

where: $$Y = \frac{P \cdot \lambda}{2U} (1 + 2 e^{-70} \cdot (\cos 70\lambda + \sin 70\lambda))$$

$$= \left(\frac{U}{4EI}\right)^{1/4}$$

Track settlement rate is proportional to the aggregate index of ballast:

$$S \propto I_a$$

C.5 WORKING EQUATION

DYNAMIC WHEEL LOAD

The steady-state load transfer factor (due to unbalance speed in curves) is given by:

$$\phi_s = 2.788\ (1.15\ E\text{-}5\ V^2D - 0.0177\ S)$$

where: V = vehicle speed (mph)

D = degree of curve (degree)

S = superelevation (inch)

The dynamic load factor (due to vehicle interaction with track roughness) is given by:

$$\phi_d = 7.94\ E\text{-}6\ V^{0.68}\ (0.585\ SI^{1.4} + 1.22\ CI)\ \left(\frac{M_u}{3165}\right)^{0.5}$$

where: SI = surface error index

CI = cross-level error index

M_u = unsprung mass

This equation is drived from a full-body vehicle dynamic model simulation for a range of track roughnesses in a sample mainline track (CWR). The validation is shown in Figure C.13. The velocity term ($V^{0.68}$) generally agrees with test data on 100-ton cars by Batelle Columbus Labs (on wood tie track) and by tests done on Canadian Railways (on concrete tie track) (see Figures C.14 and C.15, respectively).

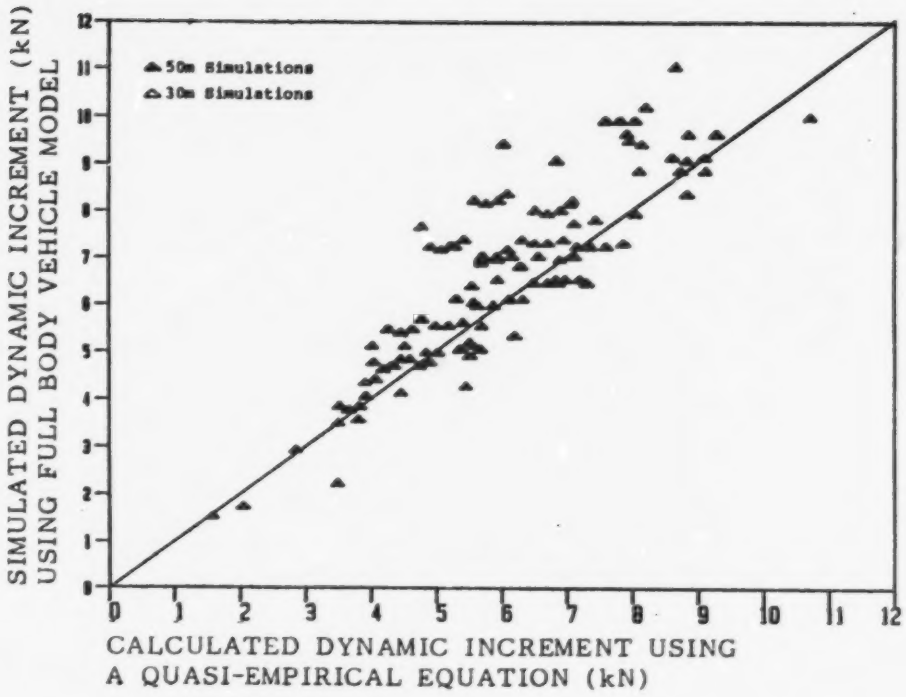

Figure C.13 Validation curve for the vehicle dynamic increment equation

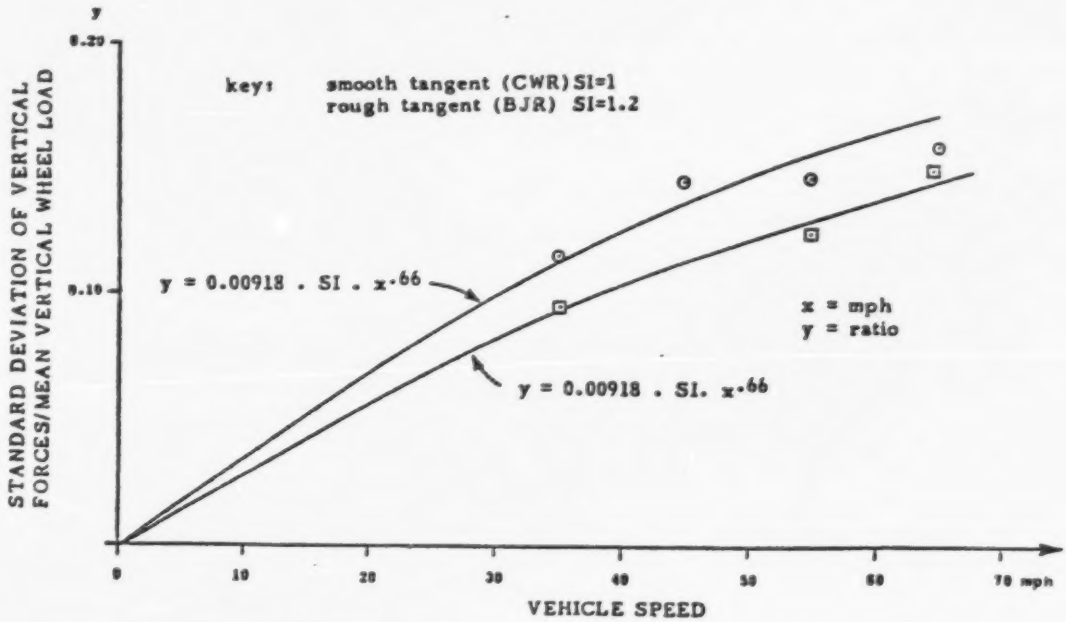

Figure C.14 Effect of speed on dynamic wheel load increment for a 100-ton car (ref. Ahlbeck et al., 1980)

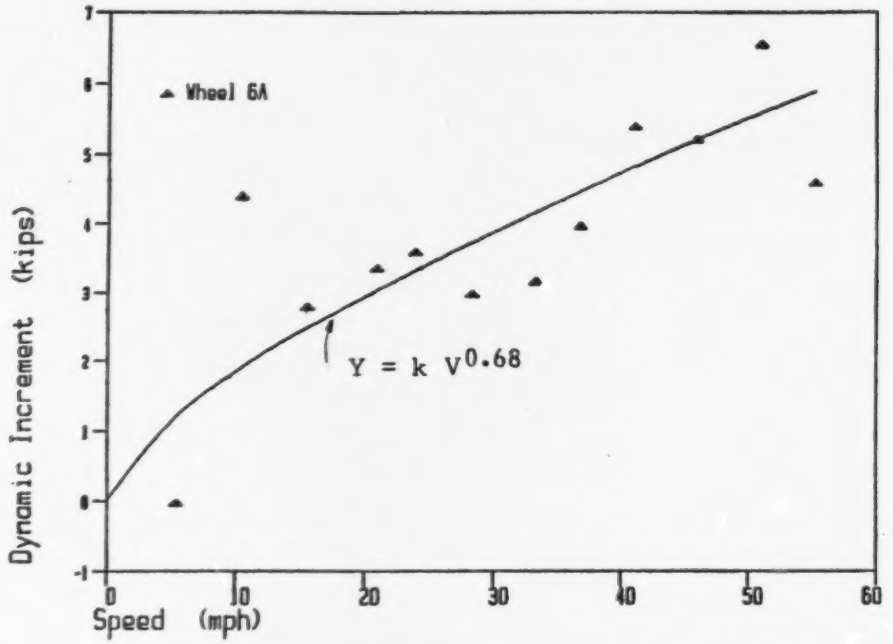

Figure C.15 Dynamic wheel force increment versus speed for 100-ton car

For other types of vehicles, similar simulation must be carried out using approporiate vehicle parameters. This work is in progress. For the present it is assumed that the above equation can be adapted to other vehicles by making an adjustment based on the unsprung mass, i.e.:

$$\phi_d = 7.94\ E\text{-}6\ V^{0.68}\ (0.585\ SI^{1.4} + 1.22\ CI)\ \left(\frac{Mu}{3165}\right)^{0.5}$$

where: Mu = unsprung mass (lb)

3156 lb = unsprung mass of a 100-ton car.

Dynamic wheel loads on high and low rails of a curve can therefore be estimated as follows (tangent track is a curve with zero degree):

- on high rail:
  $P_{Hmax} = P_o\ (1 + \phi_s)\ (1 + \phi_d)$
  $P_{Hmin} = P_o\ (1 + \phi_s)\ (1 - \phi_d)$

- on low rail:
  $P_{Lmax} = P_o\ (1 - \phi_s)\ (1 + \phi_d)$
  $P_{Lmin} = P_o\ (1 - \phi_s)\ (1 - \phi_d)$

where: P_o = static wheel load (lbs)

$P_{\substack{Hmax,Hmin \\ Lmax,Lmin}}$ = dynamic wheel load (lbs)

DIFFERENTIAL SETTLEMENT RATE

The permanent track settlement per wheel loading cycle, S, (in./cycle) is given by:

$$S = k \cdot Y^2 \cdot I_a$$

where: $y = \frac{p\lambda}{2U}(1 + 2\, e^{-70} \cdot (\cos 70\lambda + \sin 70\lambda))$

$$\lambda = \left(\frac{U}{4EI}\right)^{1/4}$$

k = constant (to be calibrated)

Y = elastic track deflection (in.)

I_a = aggregate index

P = dynamic wheel load (lb)

U = track modulus ($lb/in.^2$)

EI = rail section modulus ($lb.in^2$)

Differential track settlement (i.e. track error growth rate) per wheel loading cycle is:

$$\Delta S = \frac{k}{2}\left[(S_{Hmax} - S_{Hmin}) + (S_{Lmax} - S_{Lmin}) \right]$$

where: S_{Hmax} = maximum track settlement rate on high rail (calculated with P_{Hmax})

S_{Hmin} = minumum track settlement rate on high rail (calculated with P_{Hmin})

S_{Lmax} = maximum track settlement rate on low rail (calculated with P_{Lmax})

S_{Lmin} = minimum track settlement rate on low rail (calculated with P_{Lmin})

EQUIVALENT CYCLE

N_{ij} cycles of traffic category i running over track category j are equivalent to N_{ij}^* cycles of a reference traffic category (*) running over reference track category (*). N_{ij}^* is given by:

$$N_{ij}^* = \frac{\Delta S_{ij}}{\Delta S^*} \cdot N_{ij}$$

where: ΔS_{ij} = the differential track settlement corresponding to traffic i over track j

ΔS^* = the differential track settlement corresponding to the reference traffic/track

TOTAL EQUIVALENT CYCLE

For track length which is made up of m homogeneous categories and a traffic mix which is made up of n homogeneous traffic categories, the total equivalent cycle for all traffic running over the full track length is:

$$N^*_{total} = \sum_{i}^{n} \frac{1}{L} \sum_{j}^{m} \ell_j \cdot N_{ij}$$

where: ℓ_j = the length of track category j

L = the total track length.

CALIBRATION

From track geometry car data, track error growth characteristics can be established such as:

	Track Error (in.)	
Year since tamping	Mean	Standard Deviation
0	x_o	s_o
1	x_1	s_1
2	x_2	s_2
.	.	.
.	.	.
.	.	.
Q	x_Q	s_Q

where Q = surfacing cycle.

Based on records of traffic flow and track upgrading (if any), the actual wheel load cycle for each of these years can be normalized into equivalent cycles. A regression of track error (x,s) versus equivalent cycle, N*, can be used to obtain a track error growth function.

SURFACING CYCLE

Once the model has been calibrated, it can be used to calculate the required surfacing cycle for any future changes in track, traffic and operating conditions. Some examples of these changes are:

- track: upgrading of BJR to CWR, imposing new track geometry standards
- traffic: increasing tonnage, adding 125-ton cars
- operation: increasing speed, reducing local surfacing gang capacity.

The calculation will be more accurate if the changes are small. The general procedure is as follows:

- calculate new total number of normalized loading cycles per year, taking into account any changes in track, traffic and operating conditions
- calculate new track error growth based on the applicable track geometry standard; calculate the per cent poor track for each option of surfacing cycle (e.g. 1, 2, 3 years)

. based on the local surfacing gang capacity, select the appropriate surfacing cycle.

C.6 CONSIDERATION OF BALLAST FOULING

C.6.1 Fouling Rate

A study by CP Rail has produced an empirical relationship between traffic and ballast fouling as shown in Figure C.16. Traffic is represented by total tonnage (in millions of gross tons). Ballast fouling is represented by the reduction in the depth of the clean, free-draining ballast layer (inch). Ballast quality is represented by the aggregate index (called abrasion number by CP). An empirical curve is provided for each ballast grading. For grading number 4 (common for a main line), the mathematical expression of the empirical relationship is:

$$d = 3.73\ E\text{-}5\ (I_a)^{1.54}$$

where: d = ballast fouling rate (inch/MGT)

I_a = aggregate index.

C.6.2 Height of Lift

The above equation will be used for the present to estimate the required lift for a given surfacing cycle.

If n (year) is the surfacing cycle, and X (MGT) is the annual tonnage, the depth of fouled ballast is:

$$D_f = 3.73\ E\text{-}5\ (I_a)^{1.54} \cdot nX\ (in.)$$

A lift has to be slightly greater than D_f to compensate for the initial track settlement due to compaction. CN data (Dalton and Scott, 1983) showed that at one test site a lift of 3" was followed by an initial track settlement of 0.45". Assuming that the initial settlement is proportional to the height of the lift, the following equation is proposed for the estimation of lift:

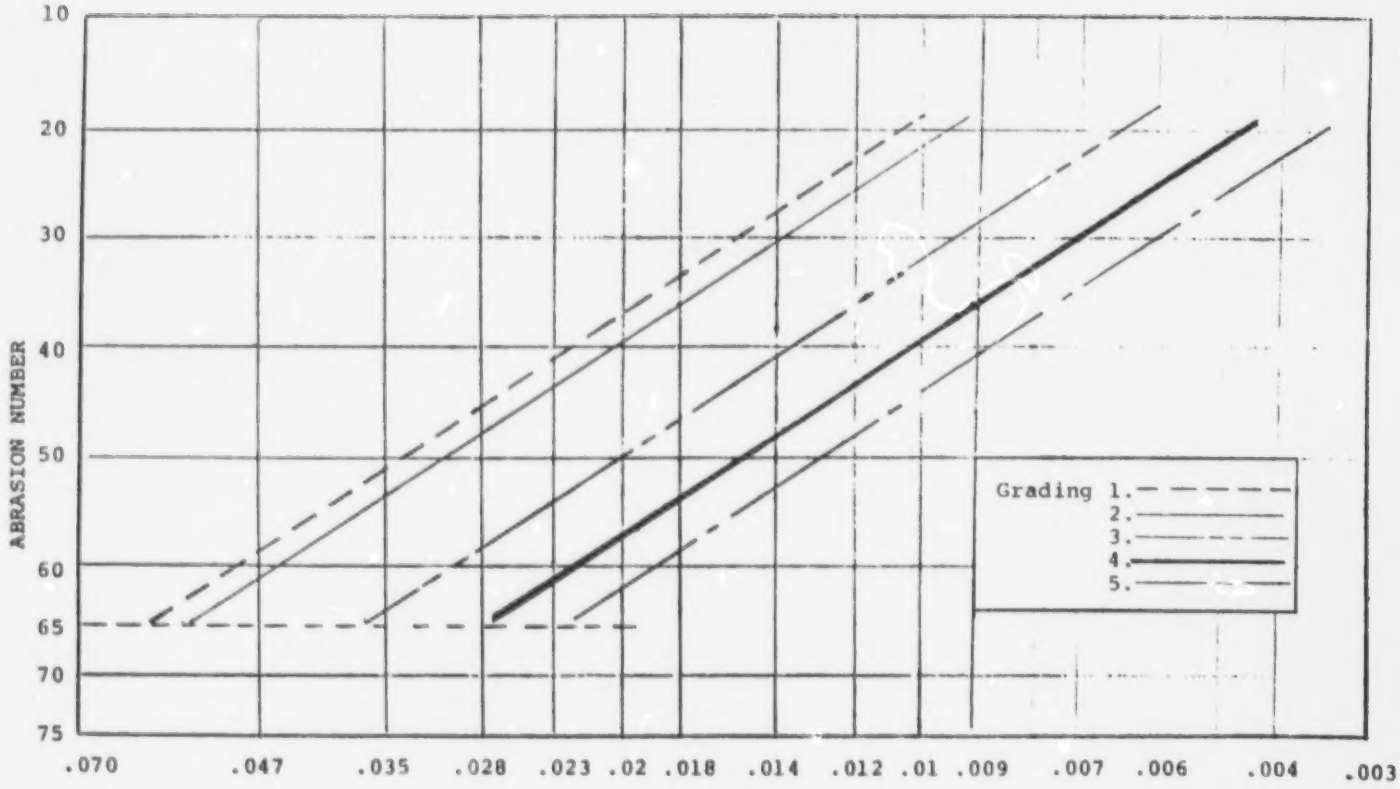

Note: Developed for tangent track with 7 in. of Ballast below tie. A small amount of contamination from outside sources has been taken into consideration.

Caution: Excessive handling of ballast materials in the upper range of Abrasion numbers may generate fines which will reduce applicable cumulative tons of rail traffic.

Figure C.16 Upper ballast deterioration rate versus abrasion number for different gradations

$$D_\ell = 1.175\ D_f$$

where: D_ℓ = height of lift (in.)

D_f = depth of ballast fouling (in.)

C.6.3 Limit of Surfacing Cycle Due to Ballast Fouling

Normally, surfacing maintenance is carried out because of track geometry error. Ballast fouling accelerates track geometry deterioration, and hence indirectly influences the surfacing cycle. The general relationship is therefore:

Although this relationship is implicitly incorporated in the calibration, the analysis of the surfacing cycle does not formally incorporate the degree of ballast fouling into the track geometry deterioration calculation. This would cause an error if the changes in track, traffic and operating conditions result in a projected new surfacing cycle which is considerably longer than the existing one. This is because the track deterioration rate in later years of the projected cycle would be higher due to a larger degree of ballast fouling compared to the rate calibrated based on data from earlier years. Further research is still needed in this area.

For a track in which the overall ballast condition is not allowed to deteriorate greatly (e.g. 6 to 8 inches of good clean ballast, surfaced every few years with a small lift of 1 to 2 inches), the above flow in the analysis will not be critical.

Experience generally indicates an optimal upper limit of lift for tamping efficiency and good ballast performance. If that is the case, the time taken to foul the corresponding ballast depth could be regarded as the upper limit of the calculated surfacing cycle. The optimal lift is usually from 2" to 4" maximum and depends on the experience of the individual track maintenance engineer.

C.7 COMPUTER PROGRAM

C.7.1 Description

The procedure for calculating surfacing cycle and height of lift is formulated in a computer program. A spread-sheet format (Lotus 1-2-3) is used for the initial version to facilitate program review and trial application on sections of railroad track. A FORTRAN version will be produced later to incorporate this model into the larger track system maintenance cost model.

Inputs include:

- traffic data (axle load, tonnage, speed, etc.)
- track data (track length, degree of curve, super-elevation, surface roughness)
- operating conditions (SPC limits, maximum allowable average per cent poor track, etc.).

The most relevant outputs are:

- surfacing cycle
- height of lift.

REFERENCES

Shenton, M.J. (1984), "Ballast Deformation and Track Deterioration," Track Technology Conference, Nottingham, U.K., July 11-13.

Dalton, C.J, and Scott, J.F. (1983), Predicting Requirements for Subballast Thickness, Progress Report No. 3, Transport Canada, Report No. TP 4350E.

Barksdale, R.D. (1972), Repeated Load Test Evaluation of Base Course Materials, Georgia Institute of Technology, Atlanta, Ga, May.

Raymond, G.P. (1985), personal communication.

Selig, E.T, and Alva-Hirtado, J.E. (1982), "Predicting Effect of Repeated Wheel Loading on Track Settlement," The Second International Heavy Haul Conference, Colorado Spring, Colo, September 25-30.

Raymond, G.P. (1979), Ballast Selection and Grading: A Summary Report, Canadian Institute of Guided Ground Transport, Report No. 79-4.

Talbot, A.N. (1920), "Stresses in Railroad Track," Proceedings of the AREA, First Progress Report, Vol. 19, 1918, pp 878-1062; ibid, Second Progress Report, Vol. 21, 1920, pp 645-814.

Scott, F.J. (1985), personal communication.

Ahbeck, D.R., et al. (1980), Measurements of Wheel/Rail Loads on Class 5 Track, FRA/ORD-80/19.

APPENDIX D

SAMPLE LOTUS 1-2-3 WORK SHEET

File name: TSM

TRACK SYSTEM MODEL

CIGGT Feb. 1986

Version 1

tot tonnage/yr
18300000

Track Category	Traffic Category	Nom. Axle Load US Ton	Unsprung Mass per Axle LB	Break Down US ton	Ave Speed MPH	Track Length Mile	Curve Degree	Superelevation Inch	Ave. Surface Error (Sigma)	Ave. Xlevel Error (Sigma)	Ave. Align. Error (Sigma)	Tie Asc Index	Tie Spacing Inch
CWR Tangent	20 ton	5.00	2425	3000000	60	350	0	0.00	161	127	48.0	1.5	21
	70 ton express	17.50	2425	2500000	90	350	0	0.00	161	127	48.0	1.5	21
	105 ton	26.25	2425	2250000	60	350	0	0.00	161	127	48.0	1.5	21
	115 ton	28.75	3142	1500000	60	350	0	0.00	161	127	48.0	1.5	21
	123 ton	30.75	3142	2000000	60	350	0	0.00	161	127	48.0	1.5	21
	128 ton (ref 1)	32.00	3142	4300000	60	350	0	0.00	161	127	48.0	1.5	21
	over 130 tons	38.50	4642	1700000	60	350	0	0.00	161	127	48.0	1.5	21
	Locomotives	32.35	8471	1050000	60	350	0	0.00	161	127	48.0	1.5	21
BJR Tangent	20 ton	5.00	2425	3000000	60	50	0	0.00	229	189	71.0	1.5	21
	70 ton express	17.50	2425	2500000	90	50	0	0.00	229	189	71.0	1.5	21
	105 ton	26.25	2425	2250000	60	50	0	0.00	229	189	71.0	1.5	21
	115 ton	28.75	3142	1500000	60	50	0	0.00	229	189	71.0	1.5	21
	123 ton	30.75	3142	2000000	60	50	0	0.00	229	189	71.0	1.5	21
	128 ton (ref 2)	32.00	3142	4300000	60	50	0	0.00	229	189	71.0	1.5	21
	over 130 tons	38.50	4642	1700000	60	50	0	0.00	229	189	71.0	1.5	21
	Locomotives	32.35	8471	1050000	60	50	0	0.00	229	189	71.0	1.5	21
Shallow curve	20 ton	5.00	2425	3000000	50	60	2	2.00	165	134	50.0	1.5	21
	70 ton express	17.50	2425	2500000	80	60	2	2.00	165	134	50.0	1.5	21
	105 ton	26.25	2425	2250000	50	60	2	2.00	165	134	50.0	1.5	21
	115 ton	28.75	3142	1500000	50	60	2	2.00	165	134	50.0	1.5	21
	123 ton	30.75	3142	2000000	50	60	2	2.00	165	134	50.0	1.5	21
	128 ton	32.00	3142	4300000	50	60	2	2.00	165	134	50.0	1.5	21
	over 130 tons	38.50	4642	1700000	50	60	2	2.00	165	134	50.0	1.5	21
	Locomotives	32.35	8471	1050000	50	60	2	2.00	165	134	50.0	1.5	21
Sharp curve	20 ton	5.00	2425	3000000	40	100	5	4.00	170	135	51.0	1.5	21
	70 ton express	17.50	2425	2500000	70	100	5	4.00	170	135	51.0	1.5	21
	105 ton	26.25	2425	2250000	40	100	5	4.00	170	135	51.0	1.5	21
	115 ton	28.75	3142	1500000	40	100	5	4.00	170	135	51.0	1.5	21
	123 ton	30.75	3142	2000000	40	100	5	4.00	170	135	51.0	1.5	21
	128 ton	32.00	3142	4300000	40	100	5	4.00	170	135	51.0	1.5	21
	over 130 tons	38.50	4642	1700000	40	100	5	4.00	170	135	51.0	1.5	21
	Locomotives	32.35	8471	1050000	40	100	5	4.00	170	135	51.0	1.5	21

Rail EI LB.IN^2	Ballast Abrasion Index	Ballast Condition Index	Track Modulus LB/IN/IN	Total Load Cycle per Yr.	Static Vload LB	SS Transfer Vload Factor	Dynamic Vload Factor (1Sigma)	HR Min Dynamic Vload (LB)	HR Max Dynamic Vload (LB)	LR Min Dynamic Vload (LB)	LR Max Dynamic Vload (LB)	Stdv State Curve Force	Flange Impact (Sigma)
2.64E+09	61	1	3000	1200000	5000	0.00	0.098	4507.62	5492.38	4507.62	5492.38	273.10	0.00
2.64E+09	61	1	3000	285714	17500	0.00	0.130	15229.57	19770.43	15229.57	19770.43	629.81	0.00
2.64E+09	61	1	3000	171429	26250	0.00	0.098	23665.02	28834.98	23665.02	28834.98	825.40	0.00
2.64E+09	61	1	3000	104348	28750	0.00	0.112	25527.35	31972.65	25527.35	31972.65	877.04	0.00
2.64E+09	61	1	3000	130081	30750	0.00	0.112	27303.17	34196.83	27303.17	34196.83	917.27	0.00
2.64E+09	61	1	3000	268750	32000	0.00	0.112	28413.05	35586.95	28413.05	35586.95	941.98	0.00
2.64E+09	61	1	3000	88312	38500	0.00	0.136	33254.52	43745.48	33254.52	43745.48	1065.64	0.00
2.64E+09	61	1	3000	64915	32350	0.00	0.186	26326.06	38373.94	26326.06	38373.94	948.84	0.00
2.64E+09	61	1	3000	1200000	5000	0.00	0.159	4206.72	5793.28	4206.72	5793.28	273.10	0.00
2.64E+09	61	1	3000	285714	17500	0.00	0.209	13842.05	21157.95	13842.05	21157.95	629.81	0.00
2.64E+09	61	1	3000	171429	26250	0.00	0.159	22085.27	30414.73	22085.27	30414.73	825.40	0.00
2.64E+09	61	1	3000	104348	28750	0.00	0.181	23557.90	33942.10	23557.90	33942.10	877.04	0.00
2.64E+09	61	1	3000	130081	30750	0.00	0.181	25196.71	36303.29	25196.71	36303.29	917.27	0.00
2.64E+09	61	1	3000	268750	32000	0.00	0.181	26220.97	37779.03	26220.97	37779.03	941.98	0.00
2.64E+09	61	1	3000	88312	38500	0.00	0.220	30048.86	46951.14	30048.86	46951.14	1065.64	0.00
2.64E+09	61	1	3000	64915	32350	0.00	0.300	22644.66	42055.34	22644.66	42055.34	948.84	0.00
2.64E+09	61	1	3000	1200000	5000	0.06	0.090	4828.52	5787.63	4268.03	5115.82	1714.52	384.02
2.64E+09	61	1	3000	285714	17500	0.31	0.124	20099.91	25809.53	10547.24	13543.31	3933.99	3221.69
2.64E+09	61	1	3000	171429	26250	0.06	0.090	25349.71	30385.06	22407.18	26858.04	5181.89	2016.10
2.64E+09	61	1	3000	104348	28750	0.06	0.103	27382.68	33660.17	24204.17	29752.98	5506.06	2208.11
2.64E+09	61	1	3000	130081	30750	0.06	0.103	29287.57	36001.74	25887.94	31822.75	5738.67	2361.72
2.64E+09	61	1	3000	268750	32000	0.06	0.103	30478.12	37465.23	26940.29	33116.36	5913.77	2457.72
2.64E+09	61	1	3000	88312	38500	0.06	0.125	35763.26	45981.08	31611.95	40643.71	6690.09	2954.95
2.64E+09	61	1	3000	64915	32350	0.06	0.171	28476.14	40210.34	25170.70	35542.82	5956.83	2484.61
2.64E+09	61	1	3000	1200000	5000	0.06	0.080	4869.52	5721.53	4326.02	5082.93	2663.40	258.64
2.64E+09	61	1	3000	285714	17500	0.59	0.118	24521.14	31063.36	6359.41	8056.09	6142.29	2563.42
2.64E+09	61	1	3000	171429	26250	0.06	0.080	25565.00	30038.05	22711.58	26685.38	8049.77	1357.88
2.64E+09	61	1	3000	104348	28750	0.06	0.092	27661.05	33237.52	24573.68	29527.74	8533.34	1487.20
2.64E+09	61	1	3000	130081	30750	0.06	0.092	29585.30	35549.70	26283.16	31581.85	8945.75	1590.65
2.64E+09	61	1	3000	268750	32000	0.06	0.092	30787.95	36994.81	27351.58	32865.66	9186.69	1655.32
2.64E+09	61	1	3000	88312	38500	0.06	0.111	36237.17	45313.96	32192.59	40256.28	10392.66	1991.55
2.64E+09	61	1	3000	64915	32350	0.06	0.152	29050.15	39473.99	25807.74	35068.13	9253.59	1673.42

Dyn. Rail Lat.Force	Dyn. Flanging Force	HR Contact Rad Sum(1/R)^2/3	LR Contact Rad Sum(1/R)^2/3	HR Contact Stress PSI	LR Contact Stress PSI	Probability of False Fls Ct.	HR Tread Force LB	LR Tread Force LB	HR Flange Force LB	HR T/P Force Ratio	LR T/P Force Ratio	HR Oct. Shear Strs Range PSI	LR Oct. Shear Strs Range PSI
273.10	546.20	0.24	0.24	98581	98581	0.00	273	273	0	0.05	0.05	33078	32499
629.81	1259.63	0.24	0.24	151018	151018	0.00	630	630	0	0.04	0.03	47297	46548
825.40	1650.81	0.24	0.24	171241	171241	0.00	825	825	0	0.03	0.03	52697	52117
877.04	1754.07	0.24	0.24	177234	177234	0.00	877	877	0	0.03	0.03	54341	53687
917.27	1834.55	0.24	0.24	181248	181248	0.00	917	917	0	0.03	0.03	55425	54771
941.98	1883.96	0.24	0.24	183669	183669	0.00	942	942	0	0.03	0.03	56078	55425
1065.64	2131.27	0.24	0.24	196737	196737	0.00	1066	1066	0	0.03	0.02	59653	58870
948.84	1897.68	0.23	0.23	182914	182914	0.00	949	949	0	0.03	0.02	55825	54814
273.10	546.20	0.24	0.24	100348	100348	0.00	273	273	0	0.05	0.05	32771	32771
629.81	1259.63	0.24	0.24	154468	154468	0.00	630	630	0	0.03	0.03	47224	47224
825.40	1650.81	0.24	0.24	174310	174310	0.00	825	825	0	0.03	0.03	52740	52740
877.04	1754.07	0.24	0.24	180797	180797	0.00	877	877	0	0.03	0.03	54421	54421
917.27	1834.55	0.24	0.24	184892	184892	0.00	917	917	0	0.03	0.03	55527	55527
941.98	1883.96	0.24	0.24	187361	187361	0.00	942	942	0	0.02	0.02	56193	56193
1065.64	2131.27	0.24	0.24	201425	201425	0.00	1066	1066	0	0.02	0.02	59871	59871
948.84	1897.68	0.23	0.23	188579	188579	0.00	949	949	0	0.02	0.02	56022	56022
2098.54	3813.04	0.24	0.27	100315	109227	0.05	1886	1886	3813	0.33	0.37	64312	77812
7175.69	11129.68	0.24	0.27	165036	151052	0.05	4349	4349	11130	0.17	0.32	77934	98996
7198.00	12379.89	0.24	0.27	174253	189734	0.05	5700	5700	12380	0.19	0.21	86275	99549
7714.17	13220.23	0.24	0.27	180295	196313	0.05	6057	6057	13220	0.18	0.20	87610	100959
8120.39	13879.05	0.24	0.27	184379	200759	0.05	6335	6505	13879	0.18	0.20	88712	102160
8371.49	14285.26	0.24	0.27	186841	203440	0.05	6505	6505	14285	0.17	0.20	89377	102884
9647.03	14337.12	0.24	0.27	200029	217800	0.05	7359	7359	14337	0.16	0.18	92425	106129
8441.44	14398.27	0.23	0.26	185783	200408	0.05	6553	6553	14398	0.16	0.18	84491	98446
2922.05	5585.45	0.24	0.24	99932	97667	0.07	3063	3063	5585	0.54	0.60	91178	96993
8705.71	14848.01	0.24	0.24	175539	113854	0.07	7064	7064	14848	0.23	0.88	95295	150535
9607.65	17457.42	0.24	0.24	173588	169652	0.07	9257	9257	17457	0.31	0.35	111065	116429
10040.54	18593.87	0.24	0.24	179538	175468	0.07	9836	9836	18594	0.30	0.33	112235	117519
10536.41	19482.16	0.24	0.24	183405	179442	0.07	10288	10288	19482	0.29	0.33	113333	118592
10842.01	20028.70	0.24	0.24	184057	181838	0.07	10565	10565	20029	0.29	0.32	113995	119239
12384.21	22776.84	0.24	0.24	199058	194545	0.07	11952	11952	22777	0.26	0.30	116748	121837
10927.01	20180.60	0.23	0.24	184643	185809	0.07	10642	10642	20181	0.27	0.30	109586	117830

TOTAL EQUIVALENT CYCLES

HR side wear	HR fatigue	LR fatigue
1717062	940143	1263375

TOTAL EQUIVALENT CYCLE

cut tie	split tie
1258235	1252378

Equiv. Cycle HR Side Wear (ref 12BT/2des)	Equiv. Cycle HR Fatigue *	Equiv. Cycle LR Fatigue *	dyn V rail seat load lb	dyn L rail seat load lb	cut stress psi	split stress psi	equivalent cut cycle	equivalent split cycle	Laeda (U/4EI)^.25	Trk Deflect per Unit P	HR Min Track Deflect (IN)	HR Max Track Deflect (IN)	HR Track Err Growth Factor
0	37008	20550	1648	82	17	118	80171	81694	0.023	5.31E-06	0.02	0.03	1.69E-02
0	30800	17205	5931	189	59	399	121063	121625	0.023	5.31E-06	0.08	0.10	2.73E-01
0	26979	15332	8650	248	85	575	126192	126431	0.023	5.31E-06	0.13	0.15	4.66E-01
0	18287	10354	9592	263	94	635	89227	89304	0.023	5.31E-06	0.14	0.17	6.36E-01
0	24428	13843	10259	275	100	678	122716	122758	0.023	5.31E-06	0.14	0.18	7.28E-01
0	52583	29812	10676	283	104	705	268740	268748	0.023	5.31E-06	0.15	0.19	7.88E-01
0	21451	12098	13124	320	127	860	119262	119046	0.023	5.31E-06	0.18	0.23	1.39E+00
0	12501	6927	11512	285	112	756	72140	72032	0.023	5.31E-06	0.14	0.20	1.34E+00
0	35817	21157	1738	82	18	123	85944	87405	0.023	5.31E-06	0.02	0.03	2.72E-02
0	30635	18096	6347	189	62	424	132842	133223	0.023	5.31E-06	0.07	0.11	4.40E-01
0	27058	15983	9124	248	89	604	135834	135916	0.023	5.31E-06	0.12	0.16	7.51E-01
0	18381	10858	10183	263	99	671	96930	96880	0.023	5.31E-06	0.12	0.18	1.03E+00
0	24586	14523	10891	275	106	716	133329	133194	0.023	5.31E-06	0.13	0.19	1.17E+00
0	52961	31284	11334	283	110	744	292005	291623	0.023	5.31E-06	0.14	0.20	1.27E+00
0	21726	12834	14085	320	136	918	131653	131222	0.023	5.31E-06	0.16	0.25	2.24E+00
0	12656	7476	12617	285	122	822	81991	81712	0.023	5.31E-06	0.12	0.22	2.16E+00
320313	422147	661506	1736	630	33	200	216972	181143	0.023	5.31E-06	0.03	0.03	1.75E-02
222605	176879	365833	7743	2153	130	792	399120	340061	0.023	5.31E-06	0.11	0.14	4.58E-01
148566	151493	223819	9116	2159	143	875	274959	237099	0.023	5.31E-06	0.13	0.16	4.82E-01
96570	97303	143115	10098	2314	156	958	191112	165200	0.023	5.31E-06	0.15	0.18	6.58E-01
126385	126726	185944	10801	2436	165	1018	260934	225818	0.023	5.31E-06	0.16	0.19	7.53E-01
268755	268751	393778	11240	2511	171	1056	568992	492735	0.023	5.31E-06	0.16	0.20	8.15E-01
100998	99308	144252	13794	2894	205	1268	244728	212907	0.023	5.31E-06	0.19	0.24	1.43E+00
65430	57870	81512	12063	2532	179	1109	147165	128024	0.023	5.31E-06	0.15	0.21	1.38E+00
469202	1286793	1625105	1716	877	27	183	158011	158386	0.023	5.31E-06	0.03	0.03	1.35E-02
296975	357598	1002032	9319	2612	110	797	389235	343303	0.023	5.31E-06	0.13	0.16	6.25E-01
209499	366704	439933	9011	2822	111	798	189175	206256	0.023	5.31E-06	0.14	0.16	4.27E-01
135823	231546	276670	9971	3012	121	872	130961	143635	0.023	5.31E-06	0.15	0.18	5.83E-01
177407	298652	356048	10665	3161	128	928	178428	196304	0.023	5.31E-06	0.16	0.19	6.67E-01
376809	629730	749746	11098	3253	133	962	388592	428307	0.023	5.31E-06	0.16	0.20	7.23E-01
140809	224956	265670	13594	3715	158	1154	165870	184883	0.023	5.31E-06	0.19	0.24	1.27E+00
131002	132496	173718	11842	3276	139	1009	99896	111121	0.023	5.31E-06	0.15	0.21	1.23E+00

LR Min Track Deflect (IN)	LR Max Track Deflect (IN)	LR Track Err Growth Factor	ave track err growth factor	TOT EQUIV CYCLE surface Equiv. Surf. cycle (ref. 1) 984664
0.02	0.03	0.02	0.02	25689
0.08	0.10	0.27	0.27	98712
0.13	0.15	0.47	0.47	101149
0.14	0.17	0.64	0.64	84067
0.14	0.18	0.73	0.73	119887
0.15	0.19	0.79	0.79	268235
0.18	0.23	1.39	1.39	155080
0.14	0.20	1.34	1.34	110000
0.02	0.03	0.03	0.03	41388
0.07	0.11	0.44	0.44	159037
0.12	0.16	0.75	0.75	162964
0.12	0.18	1.03	1.03	135443
0.13	0.19	1.17	1.17	193153
0.14	0.20	1.27	1.27	432160
0.16	0.25	2.24	2.24	249854
0.12	0.22	2.16	2.16	177224
0.02	0.03	0.01	0.02	23457
0.06	0.07	0.12	0.29	103818
0.12	0.14	0.38	0.43	93150
0.13	0.16	0.51	0.59	77419
0.14	0.17	0.59	0.67	110406
0.14	0.18	0.64	0.73	247022
0.17	0.22	1.12	1.28	142816
0.13	0.19	1.08	1.23	101301
0.02	0.03	0.01	0.01	21059
0.03	0.04	0.04	0.33	120526
0.12	0.14	0.34	0.38	82919
0.13	0.16	0.46	0.52	68916
0.14	0.17	0.53	0.60	98280
0.15	0.17	0.57	0.65	219891
0.17	0.21	1.00	1.14	127130
0.14	0.19	0.97	1.10	90174

RAIL REPLACEMENT ESTIMATE

s.wr+surf.def rail mile/yr	subsurf.fatigue rail mile/yr
20.3	2.4

TIE REPLACEMENT ESTIMATE

cut tie/yr	split tie/yr	effective SPC limit (in)
16206	29456	0.500

ESTIMATE OF SURFACING CYCLE & LIFT

allowable ave. % poor track	surfacing cycle (yrs)	ballast foul. rate (in/MGT)	req'd height of lift (in)
8.30	2.50	2.09E-02	1.13